Radboud Universiteit

Frustrations, memory, and complexity in physics and beyond

Mikhail Katsnelson

20 May 2020

Main collaborators

Tom Westerhout, Alex Kolmus, Bert Kappen, Alex Khajetoorians, Daniel Wegner and others, Radboud University

Andrey Bagrov, Olle Eriksson, Anders Bergman, Diana Iuşan and others, Uppsala University

Vladimir Mazurenko and Ilia Iakovlev, Ural Federal University

Dima Ageev and Irina Aref'eva, Steklov Mathematical Institute

Alessandro Principi, Manchester University

Eugene Koonin and Yuri Wolf, National Institutes of Health

Special thanks to Andrey Bagrov and Alex Khajetoorians for permission to use their slides on our common works and Ilia Iakovlev and Vladimir Mazurenko for sending additional pictures on structural complexity for this talk

Epigraph with explanations

All science is either physics of stamp collection (E. Rutherford)

In stamp collection we deal with history and complexity

But the same in biology, geology… To understand the origin of cats and mice we need to go billions years to the past

Fundamental physical laws are local in time and space

What are the physical mechanisms of "stamp collection"?!

Outline

Introduction

Holographic complexity

Pattern formation in physics: magnetic patterns as an example

Structural complexity from magnetic patterns to art objects

Self-induced glassiness and beyond: the role of frustration

Complexity of quantum frustrated systems

Remarks on biological complexity and evolution

Complexity

Schrödinger: life substance is "aperiodic crystal" (modern formulation – Laughlin, Pines and others – glass)

Intuitive feeling: crystals are simple, biological structures are complex

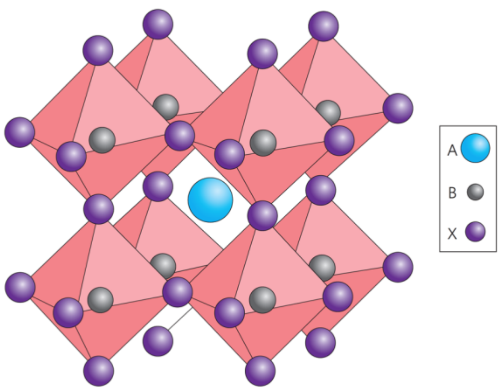

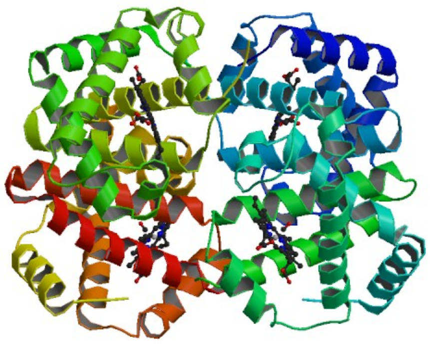

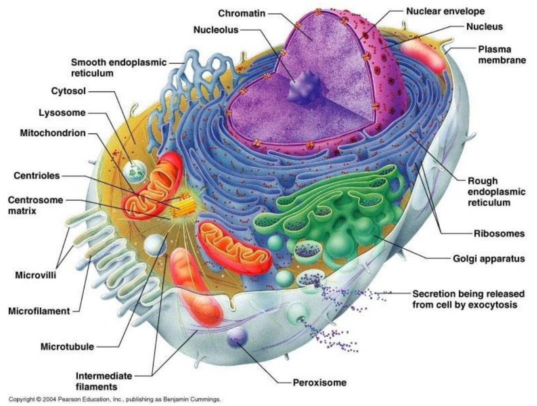

Origin and evolution of life: origin of complexity?

Complexity ("patterns") in inorganic world

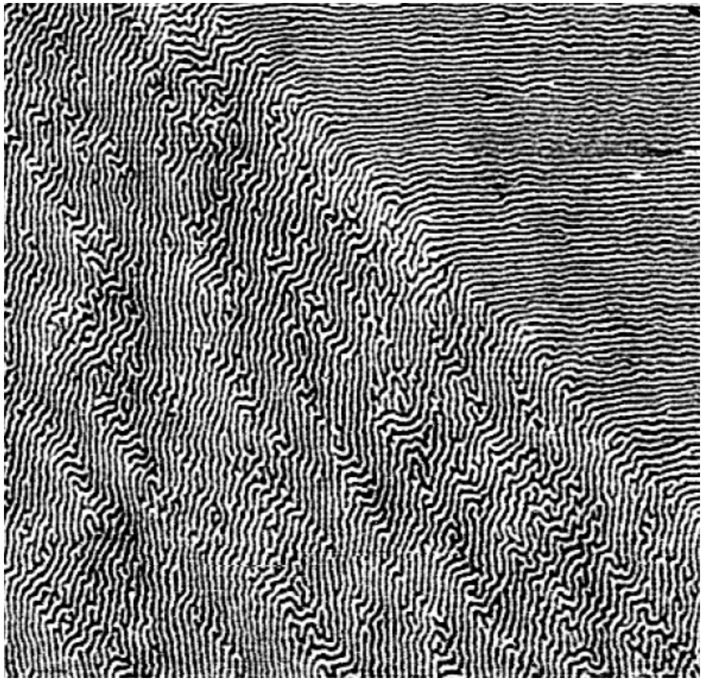

Stripe domains in ferromagnetic thin films

Stripes on a beach in tide zone

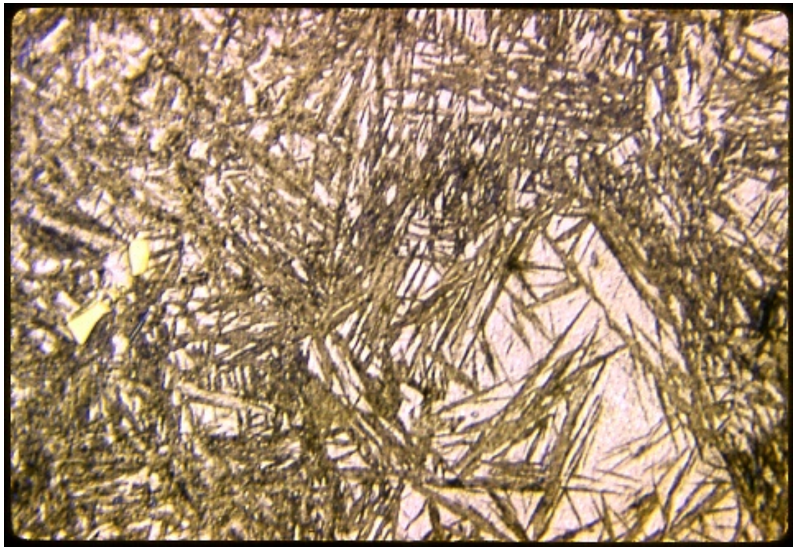

Microstructure in steel

Do we understand this? No, or, at least, not completely

What is complexity?

- Something that we immediately recognize when we see it, but very hard to define quantitatively

- S. Lloyd, “Measures of complexity: a non-exhaustive list” – 40 different definitions

- Can be roughly divided into two categories:

- computational/descriptive complexities (“ultraviolet”)
- effective/physical complexities (“infrared” or inter-scale)

Computational and descriptive complexities

- Prototype – the Kolmogorov complexity:

the length of the shortest description (in a given language) of the object of interest

- Examples:

- Number of gates (in a predetermined basis) needed to create a given state from a reference one

- Length of an instruction required by file compressing program to restore image

Descriptive complexity

- The more random – the more complex:

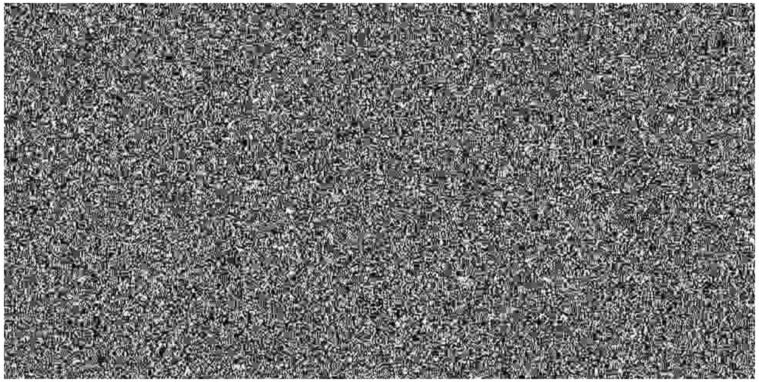

White noise
970 x 485 pixels, gray scale, 253 Kb

>

Vermeer “View of Delft”
750 x 624 pixels, colored, 234 Kb

Descriptive complexity

- The more random – the more complex:

$\gg$

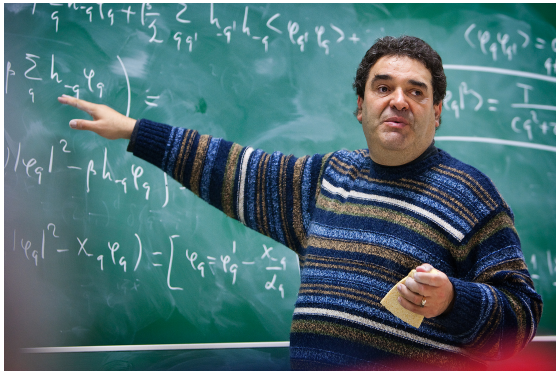

Paris japonica - 150 billion base pairs in DNA

Homo sapiens - 3.1 billion base pairs in DNA

Complexity of genomes

An idea: to take into account only part of genomes which participate in evolution

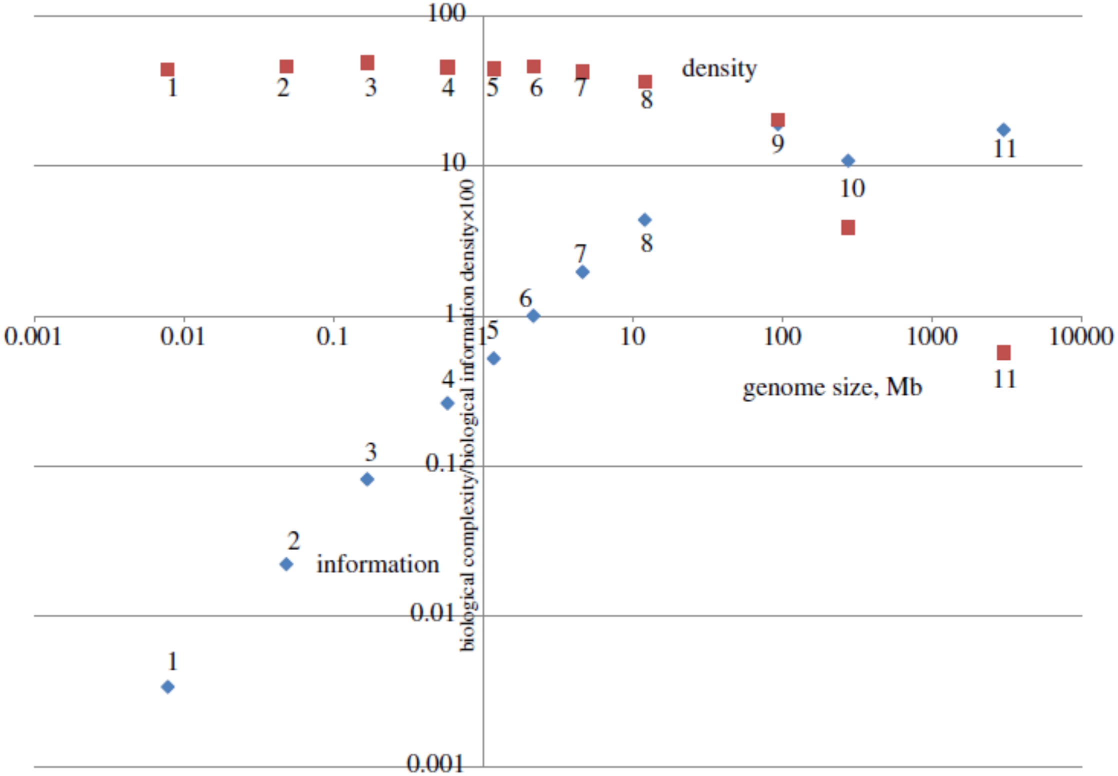

The meaning of biological information

Eugene V. Koonin

National Center for Biotechnology Information, National Library of Medicine, National Institutes of Health, Bethesda, MD, USA

Cite this article: Koonin EV. 2016 The meaning of biological information. *Phil. Trans. R. Soc. A* **374**: 20150065. http://dx.doi.org/10.1098/rsta.2015.0065

Figure 1. Biological information and information density depending on genome size: viruses, prokaryotes and eukaryotes. The biological information and density values were calculated using equations (1.4) and (1.5), respectively, and the data on genomes were from Genbank. The plot is on a double logarithmic scale. 1, encephalomyocarditis virus (RNA virus); 2, lambda phage; 3, T4 phage; 4, *Mycoplasma genitalium* (parasitic bacterium); 5, acanthamoeba polyphaga mimivirus (giant virus); 6, *Archaeoglobus fulgidus* (free-living archaeon); 7, *Escherichia coli* (free-living bacterium); 8, *Saccharomyces cerevisiae*; 9, *Arabidopsis thaliana*; 10, *Drosophila melanogaster*; 11, *Homo sapiens*. (Online version in colour.)

Effective complexity

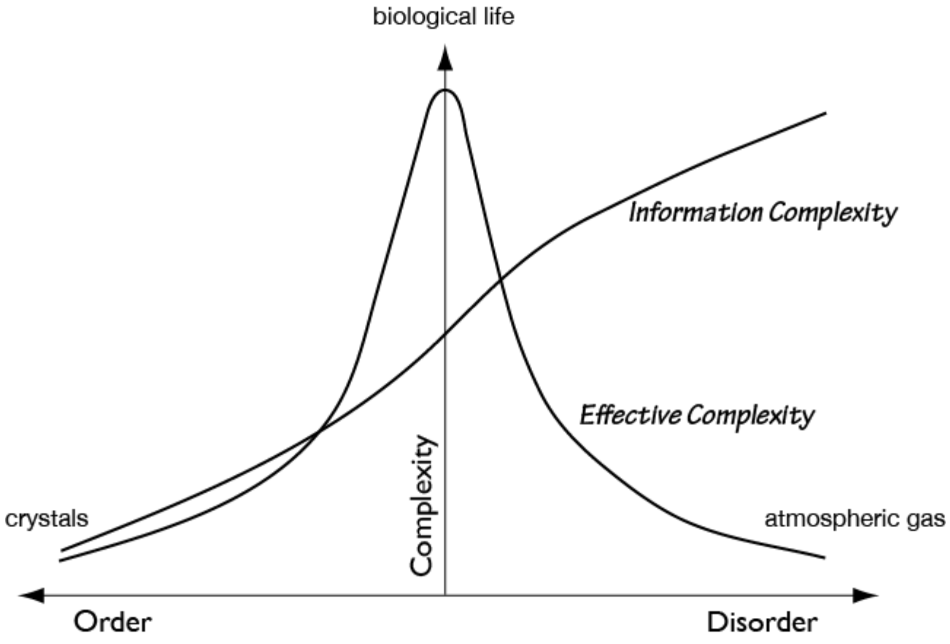

Can we come up with a quantitative measure?..

Not a mere philosophical question…

- What happens at the major evolutionary transitions?

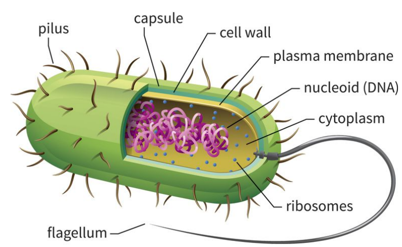

→

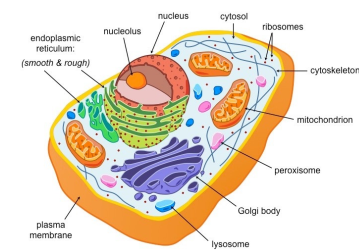

- Why are simple neural algorithms capable of solving complex many-body problems?

- Why do many natural patterns appear to be universal?

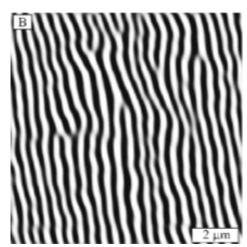

Attempts: Self-Organized Criticality

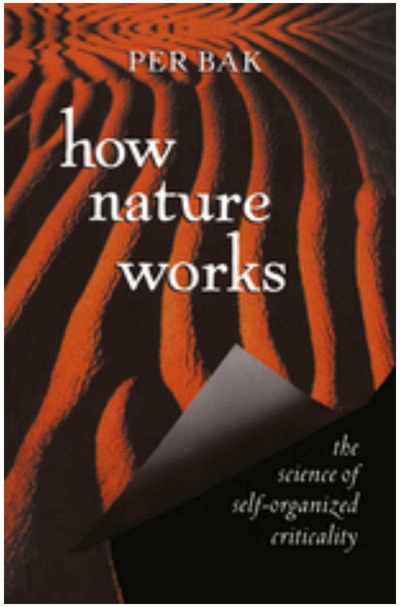

Per Bak: **Complexity *is* criticality**

Some complicated (marginally stable) systems demonstrate self-similarity and "fractal" structure

This is intuitively more complex behavior than just white noise but can we call it "complexity"?

I am not sure – complexity is hierarchical

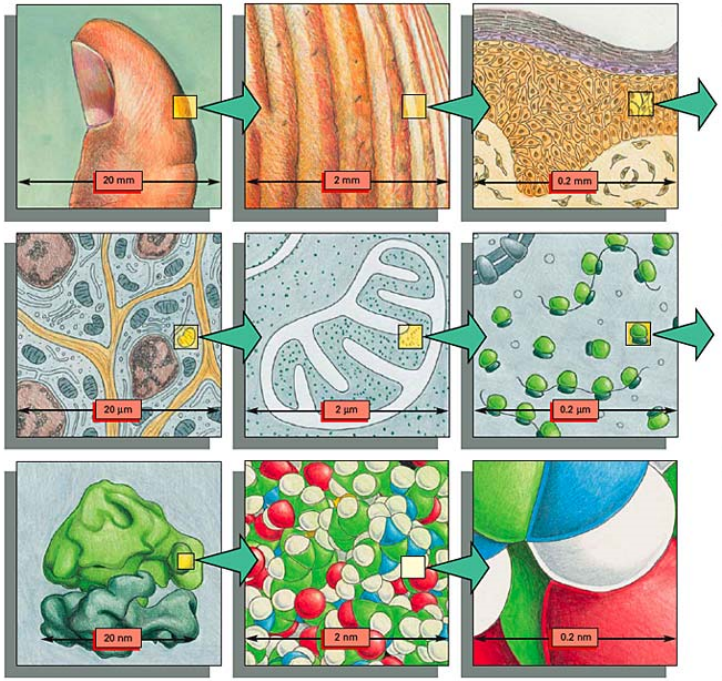

Holographic principle and complexity

“Holographic principle” emerged as an attempt to resolve the information paradox in quantum gravity (‘t Hooft 93, Susskind 94):

A state of spacetime within a given subregion can be reconstructed from the state of its boundary

The other way around:

A d-dimensional quantum field theory can in principle be equivalent to a (d+1)-dimensional theory of gravity

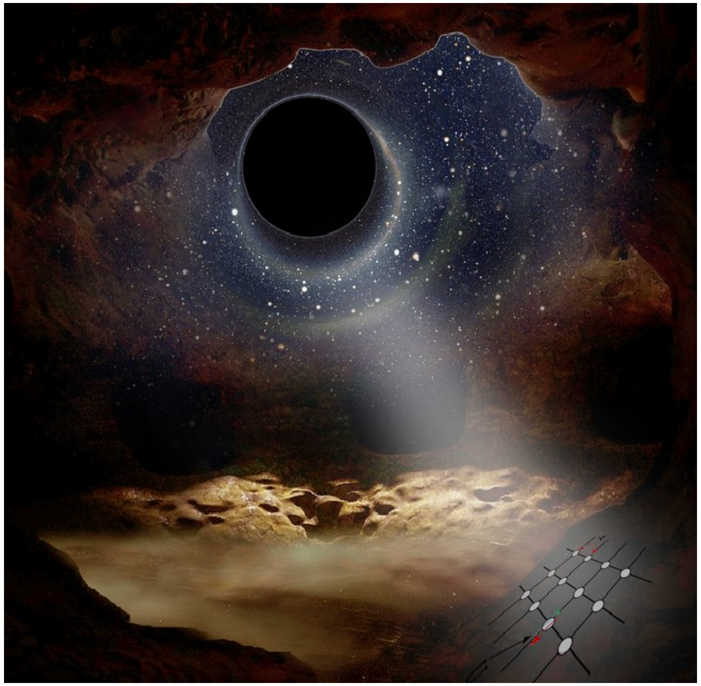

Holographic principle II

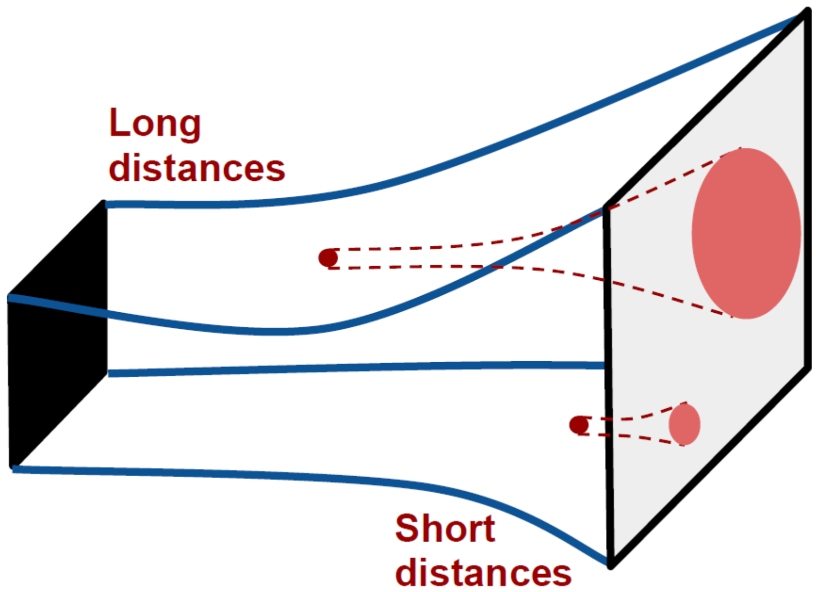

Picture from
Hartnoll, 1106.4324

Anti de
Sitter

$$ds^2 = R^2 \frac{-dx_0^2 + dx_1^2 + \cdots + dx_{d-1}^2 + dz^2}{z^2}$$

Holographic complexity

Additional coordinate: RG flow, motion along "scale" coordinate, from UV to IR

Two main definitions of holographic complexity

Complexity as volume (Susskind 2014, [https://arxiv.org/abs/1402.5674)](https://arxiv.org/abs/1402.5674)

Complexity as action (Brown et al, PRL 116, 191301 (2016))

Importantly: Both include integration over the "scale"

Holographic complexity II

JHEP

JHEP 08 (2018) 071

Holographic local quench and effective complexity

Dmitry Ageev, Irina Aref'eva, Andrey Bagrov and Mikhail I. Katsnelson

Starting with 1+1 dimensional conformal field theory (that is, scale invariant!) and creating a local quench (putting *locally* energy into the system)

Pair of solitons is formed

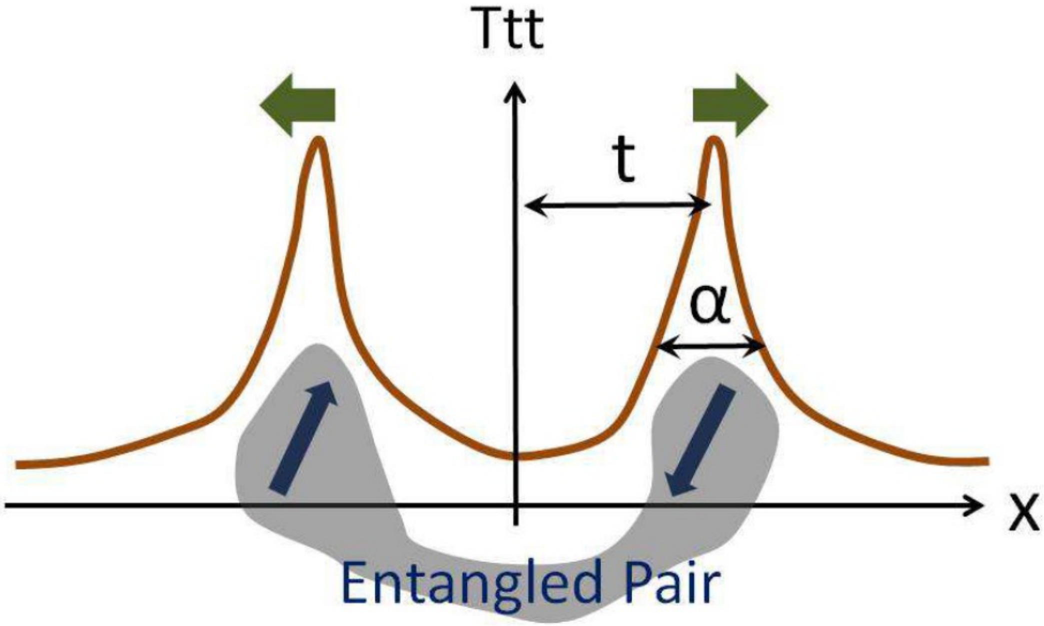

Holographic complexity III

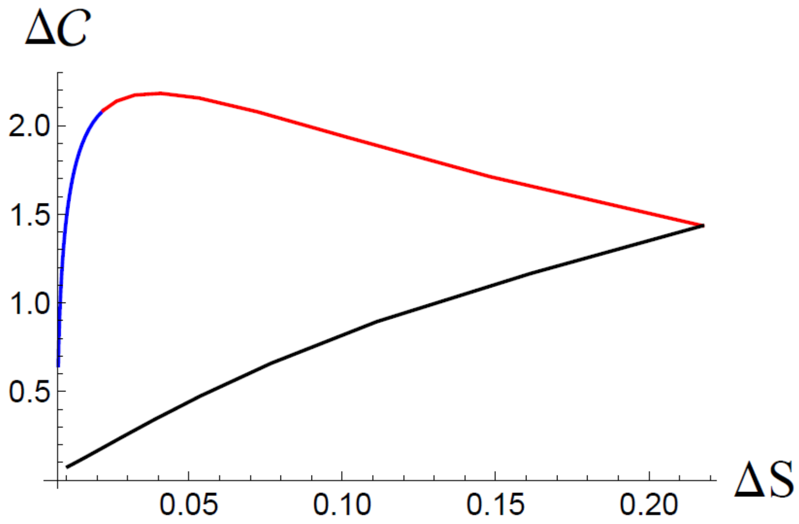

Volume complexity is a nonmonotonous function of entanglement entropy

Action complexity reaches "Lloyd computational bound", that is, the fastest production of complexity (measured as a number elementary gates) consistent with Heisenberg uncertainty principle

Holographic complexity IV

Local quench → maximally fast growth of complexity??

Criticality is not complexity but may be a prerequisite of quickly growing complexity!

Magnetic patterns

Example: strip domains in thin ferromagnetic films

PHYSICAL REVIEW B **69**, 064411 (2004)

Magnetization and domain structure of bcc $Fe_{81}Ni_{19}/Co$ (001) superlattices

R. Bručas, H. Hafermann, M. I. Katsnelson, I. L. Soroka, O. Eriksson, and B. Hjörvarsson

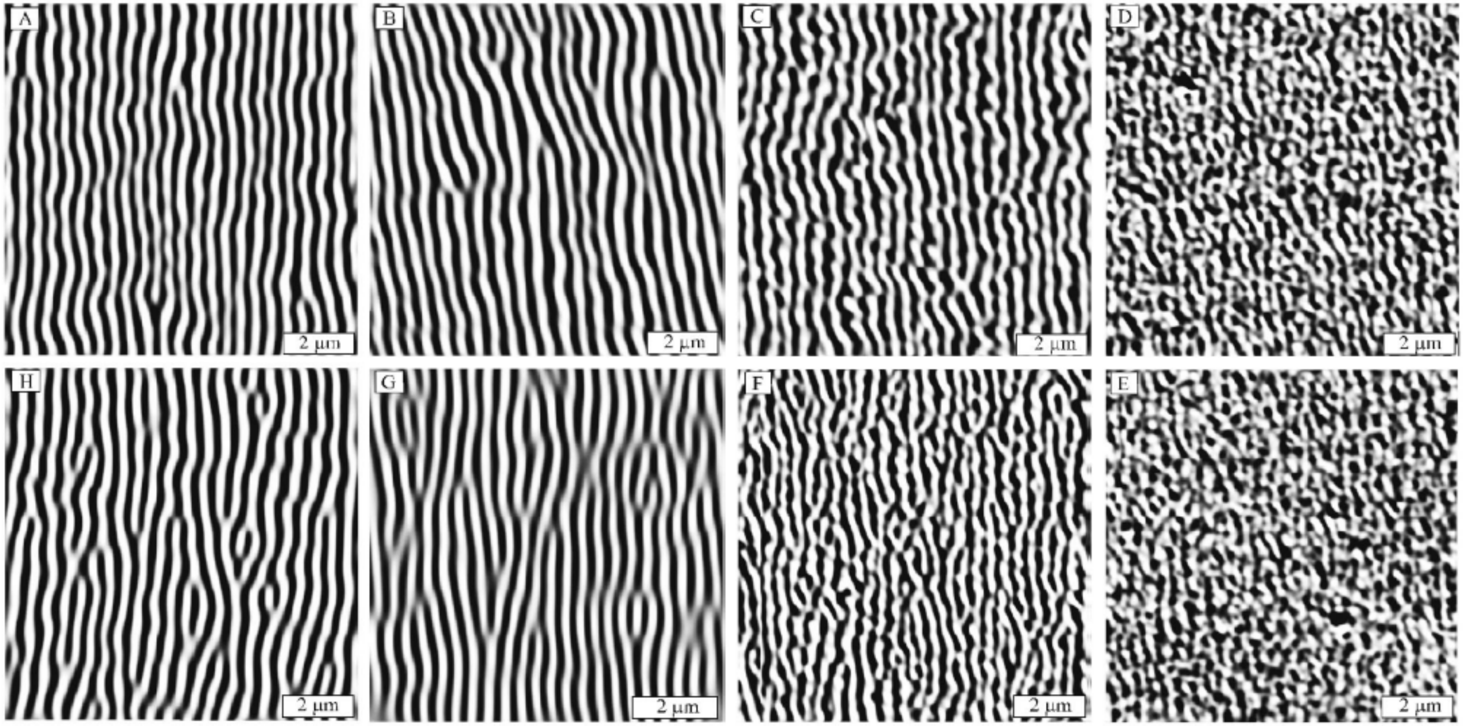

FIG. 2. The MFM images of the 420 nm thick $Fe_{81}Ni_{19}/Co$ superlattice at different externally applied in-plane magnetic fields: (a)—virgin (nonmagnetized) state; (b), (c), (d)—increasing field 8.3, 30, and 50 mT; (e), (f), (g)—decreasing field 50, 30, 8.3 mT; (h)—in remanent state.

Magnetic patterns II

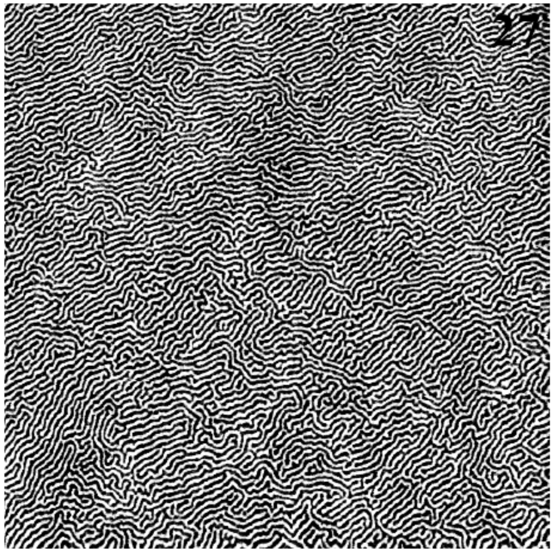

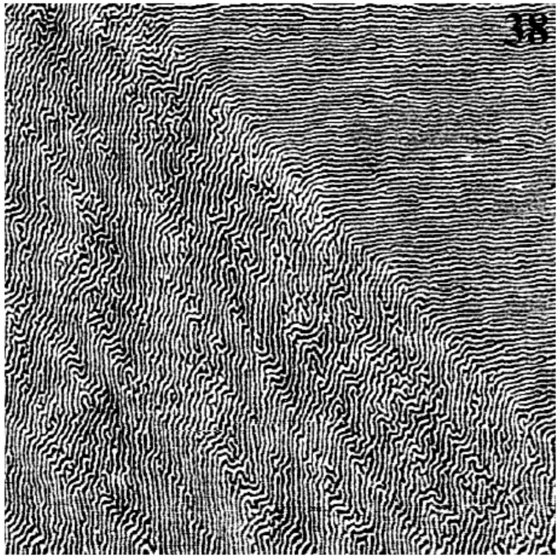

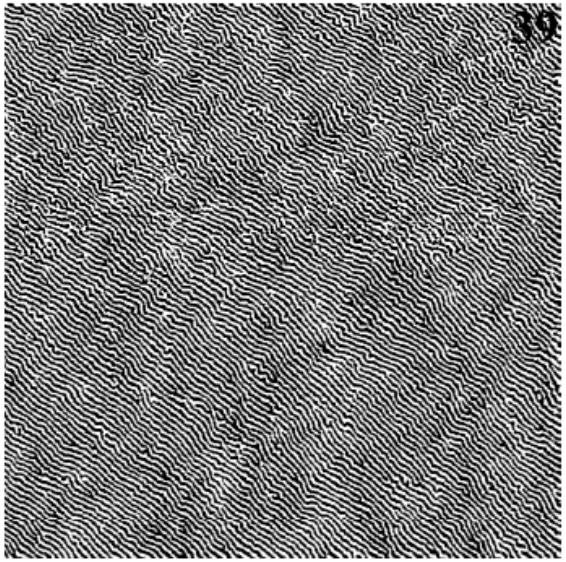

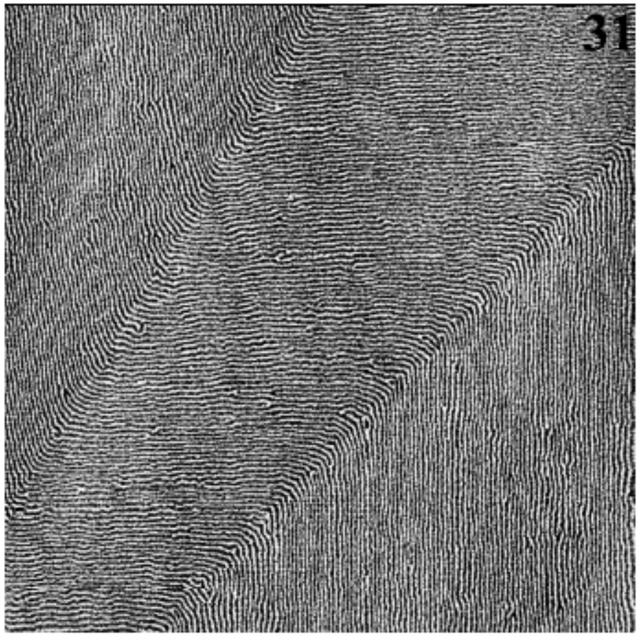

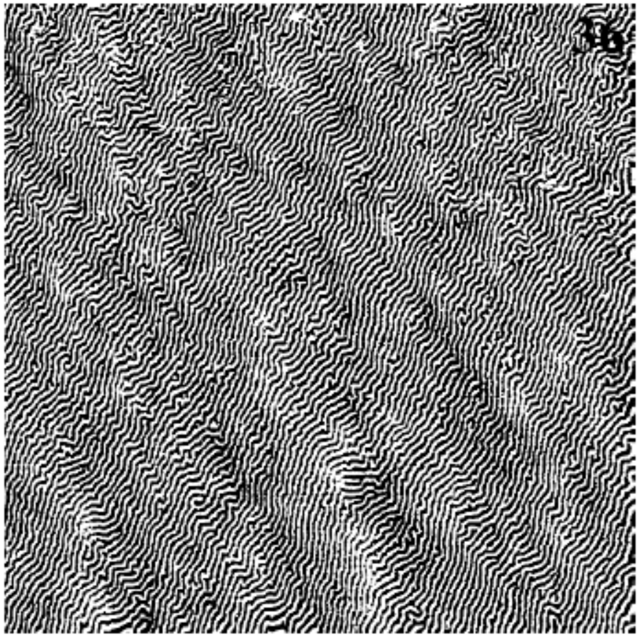

Magnetic patterns III

Europhys. Lett., **73** (1), pp. 104–109 (2006)
DOI: 10.1209/epl/i2005-10367-8

Topological defects, pattern evolution, and hysteresis in thin magnetic films

P. A. Prudkovskii[1], A. N. Rubtsov[1] and M. I. Katsnelson[2]

$$H = \int \left(\frac{J_x}{2} \left(\frac{\partial \boldsymbol{m}}{\partial x} \right)^2 + \frac{J_y}{2} \left(\frac{\partial \boldsymbol{m}}{\partial y} \right)^2 - \frac{K}{2} m_z^2 - h m_y \right) \mathrm{d}^2 r +$$

$$+ \frac{Q^2}{2} \int \int m_z(\boldsymbol{r}) \left(\frac{1}{|\boldsymbol{r} - \boldsymbol{r}'|} - \frac{1}{\sqrt{d^2 + (\boldsymbol{r} - \boldsymbol{r}')^2}} \right) m_z(\boldsymbol{r}') \mathrm{d}^2 r \mathrm{d}^2 r'.$$

Competition of exchange interactions (want homogeneous ferromagnetic state) and magnetic dipole-dipole interations (want total magnetization equal to zero)

Magnetic patterns IV

Classical Monte Carlo simulations

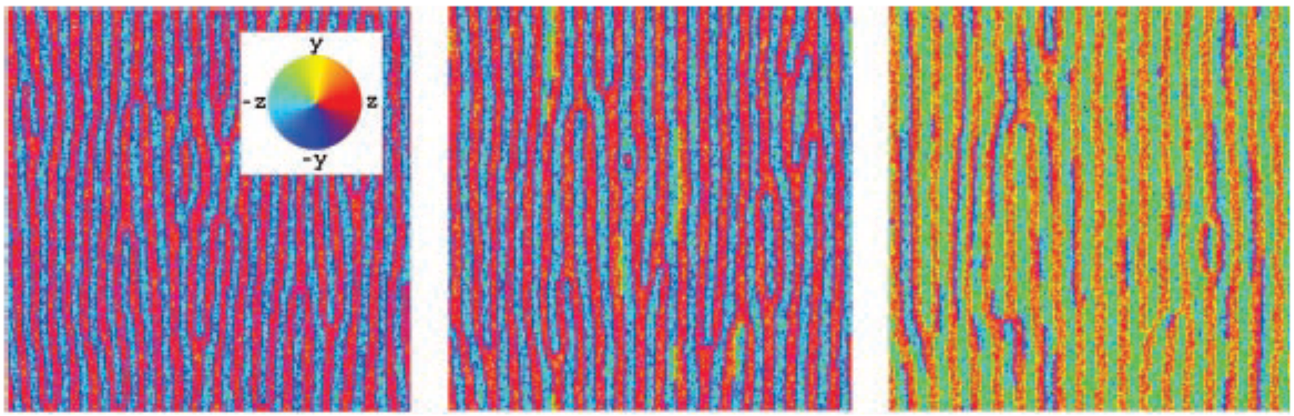

Fig. 2 – Snapshots of the stripe-domain system with the two-component order parameter at several points of the hysteresis loop for $\beta = 1$. The magnetic field is $h = 0$, $h = 0.3$, and $h = 0.6$, from left to right. The inset shows the color legend for the orientation of local magnetization.

We know the Hamiltonian and it is not very complicated

How to describe patterns and how to explain patterns?

Structural complexity

Multi-scale structural complexity of natural patterns

arXiv:2003.04632

Andrey A. Bagrov,[1,2,*] Ilia A. Iakovlev,[2,†] Mikhail I. Katsnelson,[3,2,‡] and Vladimir V. Mazurenko[2]

The idea (from holographic complexity and common sense):
Complexity is dissimilarity at various scales

Let $f(x)$ **be a multidimensional pattern**

$f_\Lambda(x)$ **its coarse-grained version (Kadanoff decimation, convolution with Gaussian window functions,…)**

Complexity is related to distances between $f_\Lambda(x)$ and $f_{\Lambda+d\Lambda}(x)$

$$\langle f(x)|g(x)\rangle = \int_D dx f(x)g(x)$$

$$\Delta_\Lambda = |\langle f_\Lambda(x)|f_{\Lambda+d\Lambda}(x)\rangle - \frac{1}{2}\left(\langle f_\Lambda(x)|f_\Lambda(x)\rangle + \langle f_{\Lambda+d\Lambda}(x)|f_{\Lambda+d\Lambda}(x)\rangle\right)| = \frac{1}{2}|\langle f_{\Lambda+d\Lambda}(x) - f_\Lambda(x)|f_{\Lambda+d\Lambda}(x) - f_\Lambda(x)\rangle|,$$

$$\mathcal{C} = \sum_\Lambda \frac{1}{d\Lambda}\Delta_\Lambda \to \int |\langle \frac{\partial f}{d\Lambda}|\frac{\partial f}{d\Lambda}\rangle| d\Lambda, \text{ as } d\Lambda \to 0$$

Structural complexity II

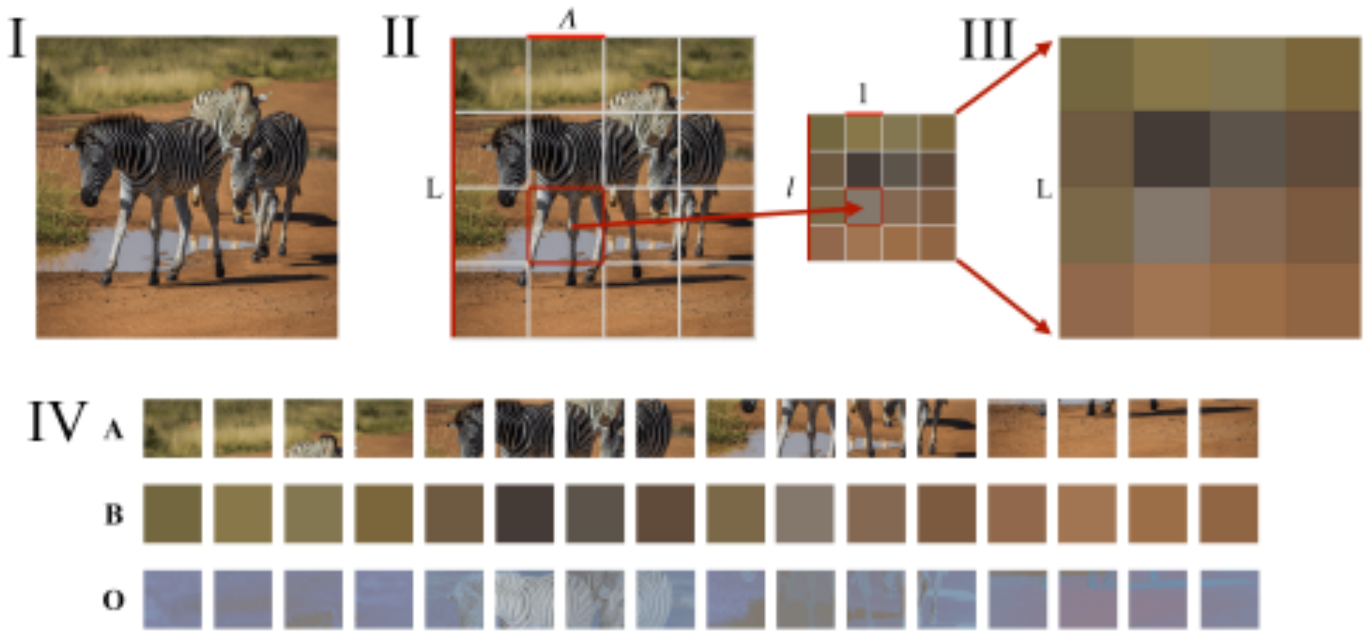

FIG. 1. Schematic representation of the idea behind the proposed method. A photo of $L \times L$ pixels (panel I) taken from www.pexels.com is divided into blocks of $\Lambda \times \Lambda$ pixels (panel II). A renormalized photo of $l \times l$ pixels is plotted, where $l = L/\Lambda$ (l=4 in this example). The renormalized photo is rescaled up to initial photo size (panel III). Vectors **A** and B are constructed from blocks of the initial and the renormalized images respectively (panel IV). The scalar product of these vectors is used to define overlap O. For illustrative purposes, pixelwise products of **A**- and B-blocks are shown as vector **O**.

Structural complexity III

Can be used as a numerical tool to find T_C from finite-size simulations: 2D Ising model

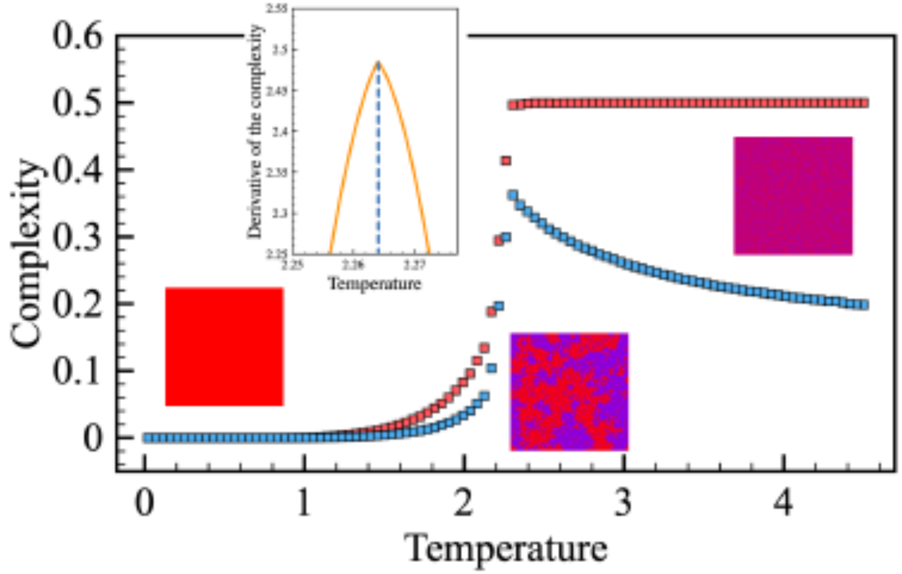

FIG. 2. Temperature dependence of the complexity obtained from the two-dimensional Ising model simulations. Red and blue squares correspond to the complexities calculated with $k \geq 0$ and $k \geq 1$, respectively. The size of error bars is smaller than the symbol size. Inset shows the first derivative of the complexity used for accurate detection of the critical temperature. Here we used $N = 8$, $\Lambda = 2$.

Structural complexity IV

3D Ising model, cubic lattice (insert shows temperature derivative of Complexity)

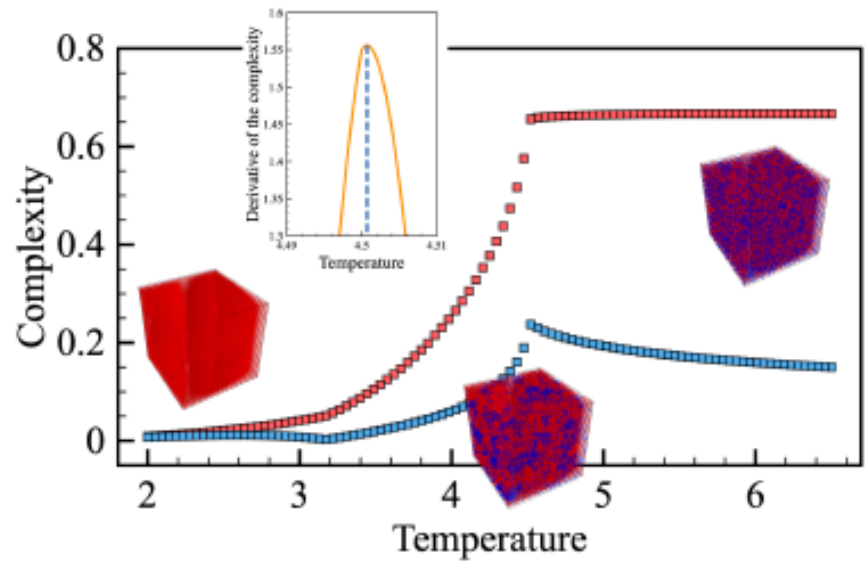

FIG. 3. Temperature dependence of the complexity obtained from the three-dimensional Ising model simulations with $\Lambda = 2$. Red and blue squares correspond to the complexities calculated with $k \geq 0$ and $k \geq 1$, respectively. The size of error bars is smaller than the symbol size. Inset shows the first derivative of the complexity used for accurate detection of the critical temperature. Here we used $L \times L \times L$ cubic lattice with $L = 256$, $N = 6$. The small but visible cusp on the blue curve around $T \simeq 3.2$ reflects the emergence of magnetic domains within the ferromagnetic phase, which takes place sometimes during MC simulations on large lattices.

Structural complexity V

Spin textures due to competition of exchange and Dzialoshinskii-Moriya interactions

$$H = -J \sum_{nn'} \mathbf{S}_n \mathbf{S}_{n'} - \mathbf{D} \sum_{nn'} [\mathbf{S}_n \times \mathbf{S}_{n'}] - \sum_{n} B S_n^z$$

FIG. 5. Configurations of the DM magnetic on 1024×1024 square lattice obtained from independent Monte Carlo runs with parameters $B = 0.05J$, $|\mathbf{D}| = J$, $T = 0.02J$. While they are visually distinct, corresponding complexities (left to right) are equal to $\mathcal{C} = 0.4992115$, $\mathcal{C} = 0.4991825$ and $\mathcal{C} = 0.4991805$.

Structural complexity VI

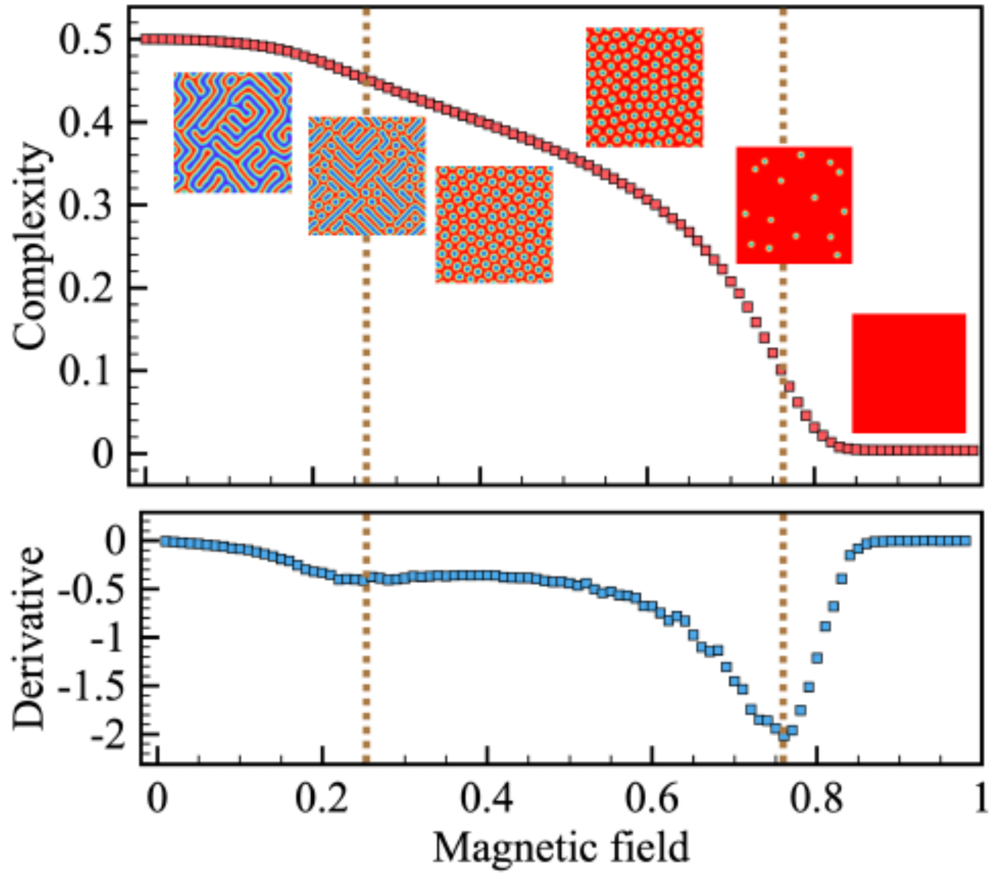

FIG. 4. (a) Magnetic field dependence of the complexity obtained from the simulations with spin Hamiltonian containing DM interaction with $J = 1$, $|\mathbf{D}| = 1$, $T = 0.02$. The error bars are smaller than the symbol size. (b) Complexity derivative we used for accurate detection of the phases boundaries.

Solution of an ink drop in water

Entropy should grow, but complexity is not! And indeed…

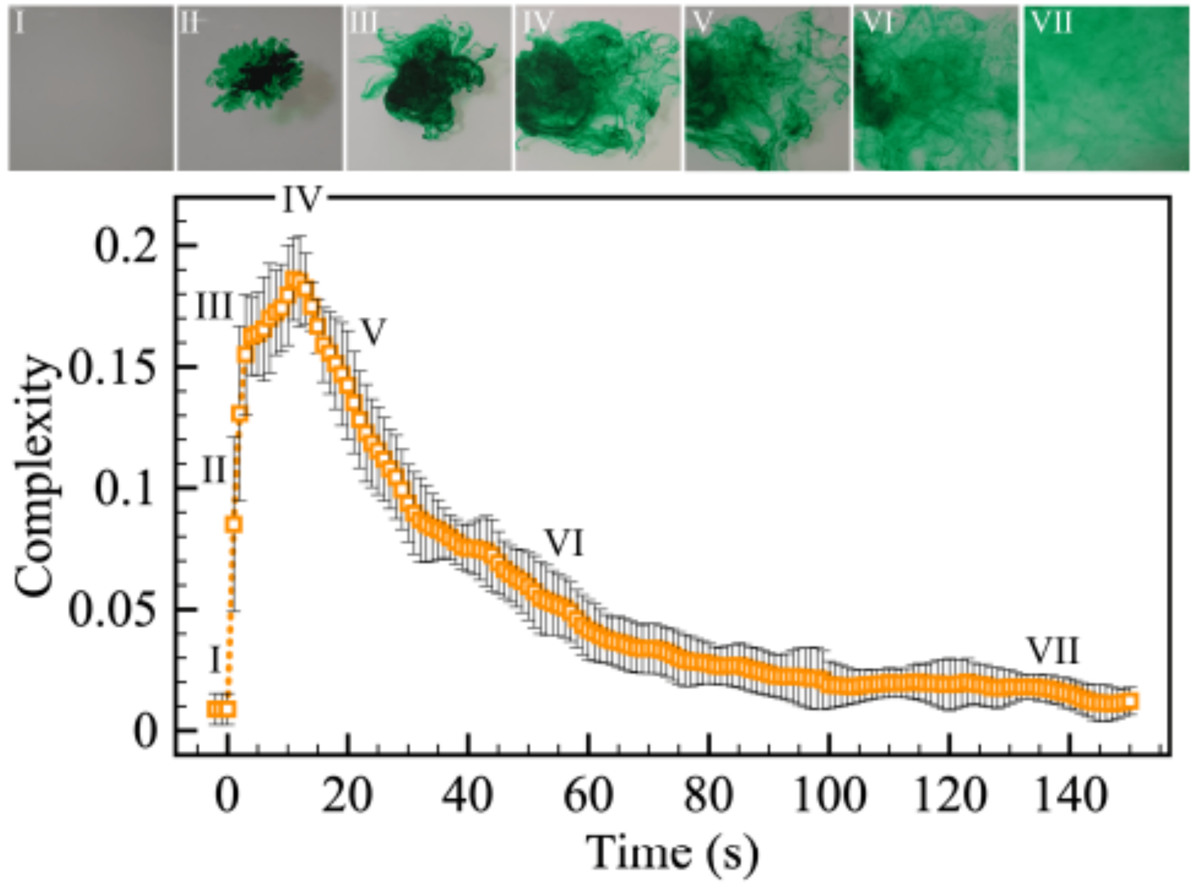

FIG. 7. The evolution of the complexity during the process of dissolving a food dye drop of 0.3 ml in water at 31°C.

Art objects (and walls)

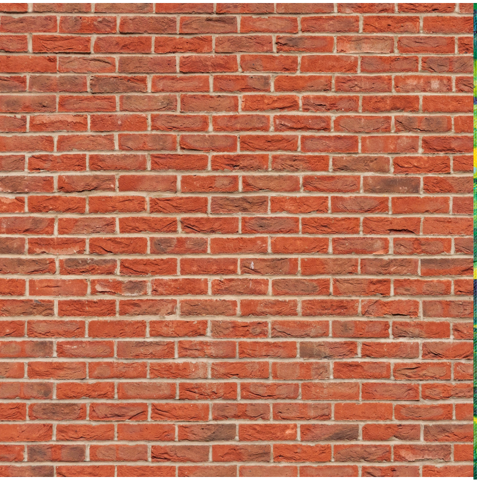

$C = 0.1076$

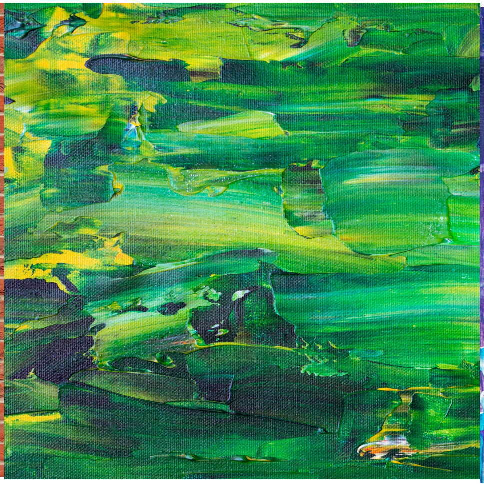

$C = 0.2010$

$C = 0.2147$

$C = 0.2765$

$C = 0.4557$

$C = 0.4581$

$C = 0.4975$

$C = 0.5552$

Competing interactions and self-induced spin glasses

Special class of patterns: "chaotic" patterns

PHYSICAL REVIEW B **69**, 064411 (2004)

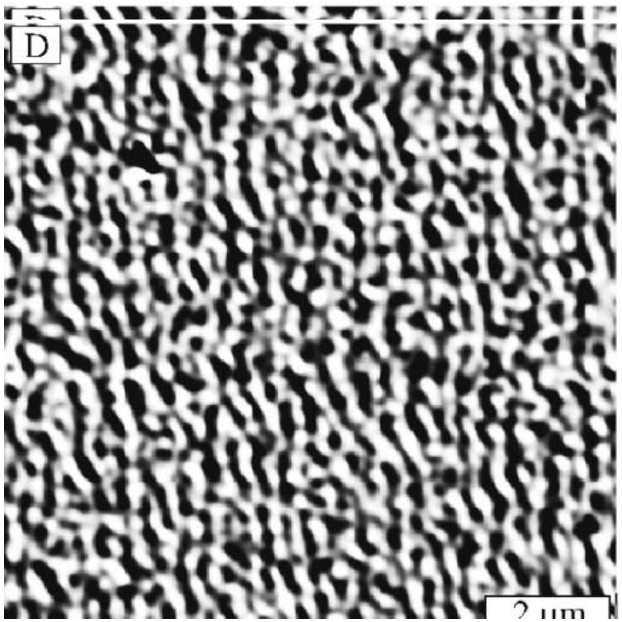

Hypothesis: a system wants to be modulated but cannot decide in which direction

$$E_m = \int\int d\mathbf{r}d\mathbf{r}' m(\mathbf{r})m(\mathbf{r}')\left[\frac{1}{|\mathbf{r}-\mathbf{r}'|} - \frac{1}{\sqrt{(\mathbf{r}-\mathbf{r}')^2+D^2}}\right]$$

$$= 2\pi \sum_{\mathbf{q}} m_{\mathbf{q}} m_{-\mathbf{q}} \frac{1-e^{-qD}}{q}, \quad (13)$$

where $m_{\mathbf{q}}$ is a two-dimensional Fourier component of the magnetization density. At the same time, the exchange energy can be written as

$$E_{exch} = \frac{1}{2}\alpha \sum_{\mathbf{q}} q^2 m_{\mathbf{q}} m_{-\mathbf{q}}, \quad (14)$$

so there is a finite value of the wave vector $q = q^*$ found from the condition

$$\frac{d}{dq}\left(2\pi \frac{1-e^{-qD}}{q} + \frac{1}{2}\alpha q^2\right) = 0 \quad (15)$$

Self-induced spin glasses II

PHYSICAL REVIEW B **93**, 054410 (2016)

Stripe glasses in ferromagnetic thin films

Alessandro Principi* and Mikhail I. Katsnelson

PRL **117,** 137201 (2016) PHYSICAL REVIEW LETTERS week ending 23 SEPTEMBER 2016

Self-Induced Glassiness and Pattern Formation in Spin Systems Subject to Long-Range Interactions

Alessandro Principi* and Mikhail I. Katsnelson

Development of idea of stripe glass, J. Schmalian and P. G. Wolynes, PRL 2000

Glass: **a system with an energy landscape characterizing by infinitely many local minima, with a broad distribution of barriers, relaxation at "any" time scale and aging (at thermal cycling you never go back to *exactly* the same state)**

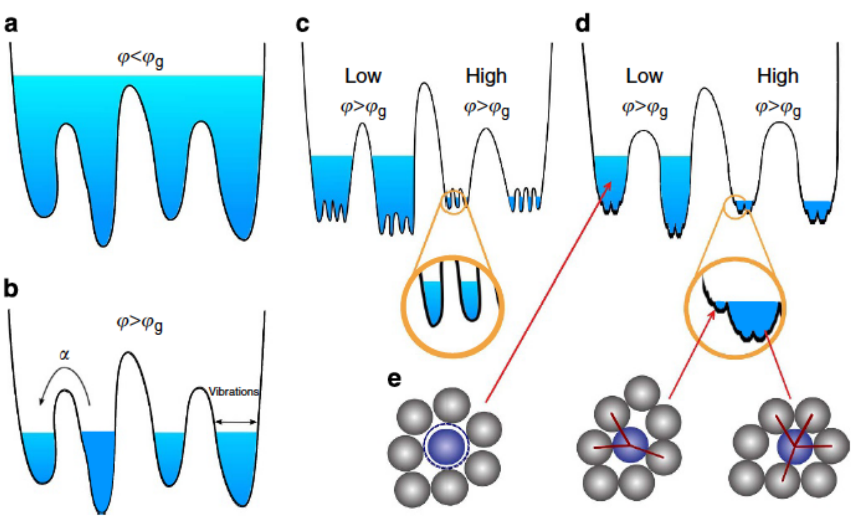

Picture from P. Charbonneau et al,

DOI: 10.1038/ncomms4725

Intermediate state between equilibrium and non-equilibrium, opportunity for history and memory ("stamp collection")

Self-induced spin glasses III

One of the ways to describe: R. Monasson, PRL 75, 2847 (1995)

$$\mathcal{H}_\psi[m,\lambda] = \mathcal{H}[m,\lambda] + g \int dr [m(r) - \psi(r)]^2$$

The second term describes attraction of our physical field $m(r)$

to some external field $\psi(r)$

If the system an be glued, with infinitely small interaction *g*, to macroscopically large number of configurations it should be considered as a glass

Then we calculate $F_g = \frac{\int \mathcal{D}\psi Z[\psi] F[\psi]}{\int \mathcal{D}\psi Z[\psi]}$ and see whether the limits

$F_{eq} = \lim_{N\to\infty} \lim_{g\to 0} F_g$ and $F = \lim_{g\to 0} \lim_{N\to\infty} F_g$ are different

If yes, this is self-induced glass

No disorder is needed (contrary to traditional view on spin glasses)

Self-induced spin glasses IV

PHYSICAL REVIEW B **93**, 054410 (2016)

Stripe glasses in ferromagnetic thin films

Alessandro Principi* and Mikhail I. Katsnelson

$$\mathcal{H}[\boldsymbol{m},\lambda] = \int d\boldsymbol{r}\{J[\partial_i m_j(\boldsymbol{r})]^2 - K m_z^2(\boldsymbol{r}) - 2\boldsymbol{h}(\boldsymbol{r})\cdot\boldsymbol{m}(\boldsymbol{r})\}$$
$$+ \frac{Q}{2\pi}\int d\boldsymbol{r}d\boldsymbol{r}' m_z(\boldsymbol{r})$$
$$\times \left[\frac{1}{|\boldsymbol{r}-\boldsymbol{r}'|} - \frac{1}{\sqrt{d^2+|\boldsymbol{r}-\boldsymbol{r}'|^2}}\right] m_z(\boldsymbol{r}')$$
$$+ \int d\boldsymbol{r}\{\lambda(\boldsymbol{r})[\boldsymbol{m}^2(\boldsymbol{r}) - 1]\}. \quad (1)$$

Self-consistent screening approximation for spin propagators

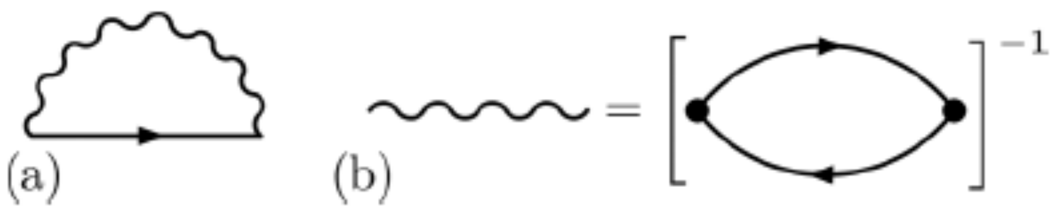

Self-induced spin glasses V

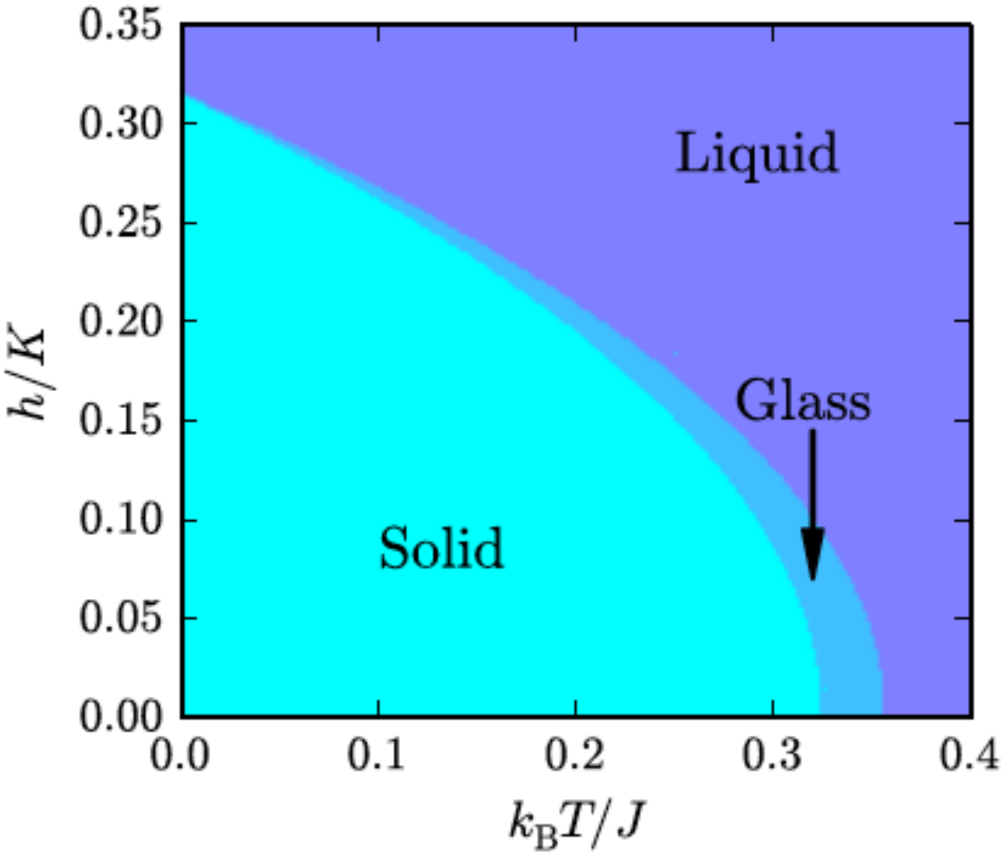

Maximum at

$$q_0 \simeq [Q/(2J)]^{1/3} \neq 0$$

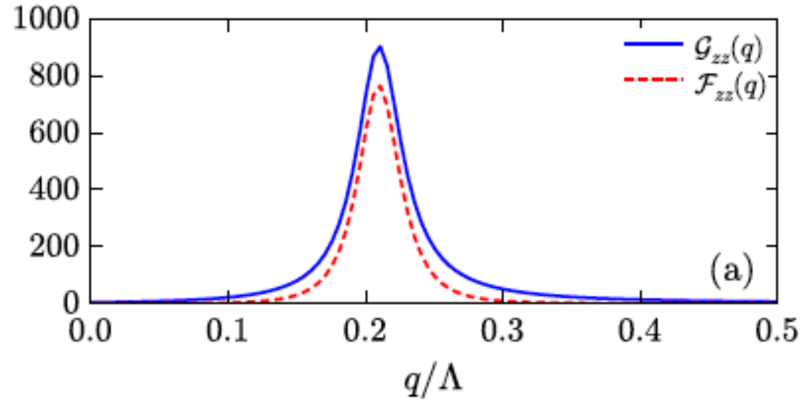

Phase diagram

q-dependence of normal and anomalous ("glassy", non-ergodic spin-spin correlators

Self-induced spin glasses VI

PRL **117,** 137201 (2016) PHYSICAL REVIEW LETTERS week ending 23 SEPTEMBER 2016

Self-Induced Glassiness and Pattern Formation in Spin Systems Subject to Long-Range Interactions

Alessandro Principi* and Mikhail I. Katsnelson

Maximal simplification (Brazovskii model)

$$\mathcal{F} = \frac{1}{2}\sum_{q} G_0^{-1}(\boldsymbol{q}) \boldsymbol{s}_{\boldsymbol{q}} \cdot \boldsymbol{s}_{-\boldsymbol{q}} + i\sum_{i} \sigma_i (s_i^2 - 1)$$

$$G_0^{-1}(\boldsymbol{q}) = q_0^D (q^2/q_0^2 - 1)^2/4 + q_0^D \varepsilon_0^2 \sin^2(\theta_{\boldsymbol{q}})$$

Spin-glass state exists!

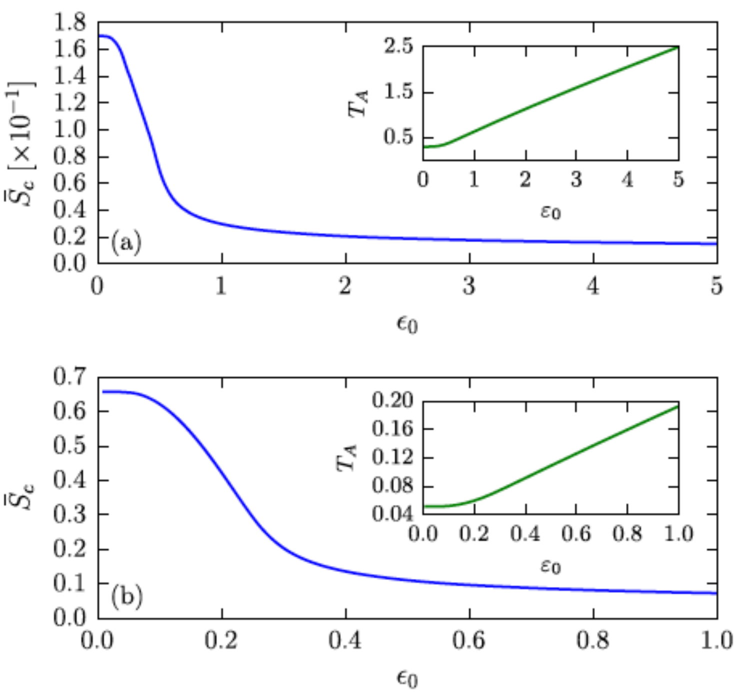

FIG. 2. Panel (a) the configurational entropy of the mean-field problem for the two-dimensional Ising model ($D = 2$ and $N_s = 1$). Note that this curve has been multiplied by a factor 0.1. Inset: the transition temperature T_A as a function of the anisotropy parameter ε_0. Panel (b) same as panel (a) but for the two-dimensional Heisenberg model ($D = 2$, $N_s = 3$). Inset: the temperature T_A as a function of ε_0.

Experimental observation of self-induced spin glass state: elemental Nd

Unconventional spin glass state in elemental neodymium in the absence of extrinsic disorder

Umut Kamber[1], Anders Bergman[2], Andreas Eich[1], Diana Iuşan[2], Manuel Steinbrecher[1], Nadine Hauptmann[1], Lars Nordström[2], Mikhail I. Katsnelson[1], Daniel Wegner[1], Olle Eriksson[2,3], Alexander A. Khajetoorians[1,*]

arXiv:1907.02295

Spin-polarized STM experiment, Radboud University

The historical conundrum

Unfortunately, the understanding of the magnetic properties of Nd has been an unsolved puzzle for almost 50 years. *Neutron diffraction investigations of the magnetic structure of Nd starting by Moon, Cable and Koehler and others are numerous. In addition there has been a recent x-ray investigation.* These revealed that Nd has the most complicated magnetic structure known for any pure element*—including a sinusoidal ordering. The reason for the found complexity has previously not been understood, basically because the magnetic interactions were not determined.*

P. A. Lindgard, T. Chatterji, K. Prokes, V. Sikolenko and J. U. Hoffmann, J Phys-Condens Mat **19** (28) (2007).

Nd(0001): electronic properties

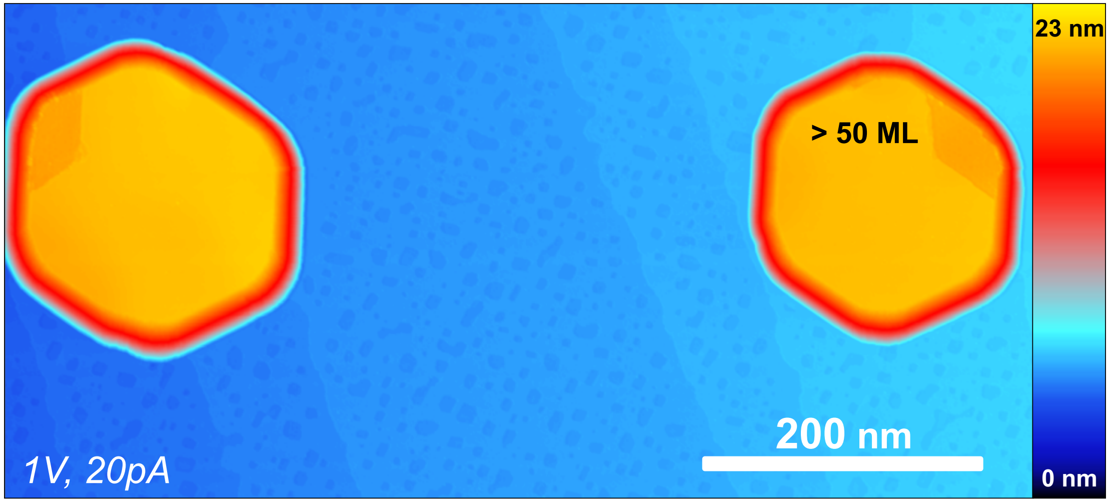

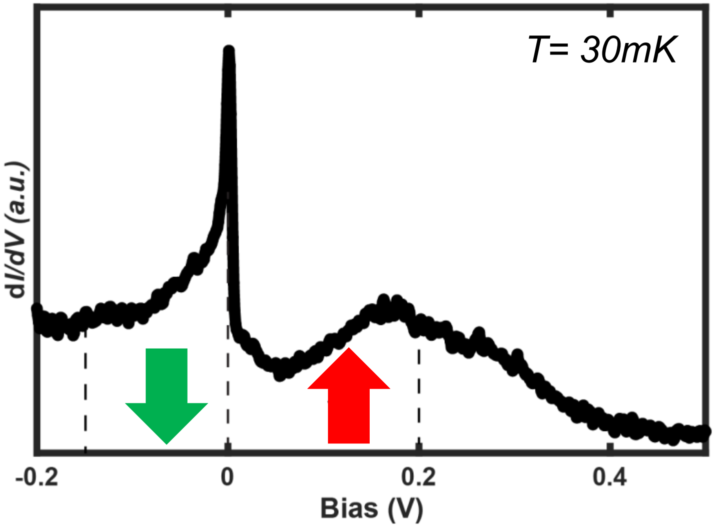

- Exchange split surface state
  - Spin contrast at each voltage with contrast inversion
- Use Cr bulk tip – out of plane contrast

D. Wegner *et al.*, *Phys. Rev. B* **73**, 165415 (2006)
D. Wegner *et al.*, *Jpn. J. Appl. Phys.* **45**, 1941 (2006)

Magnetic structure: no long-range

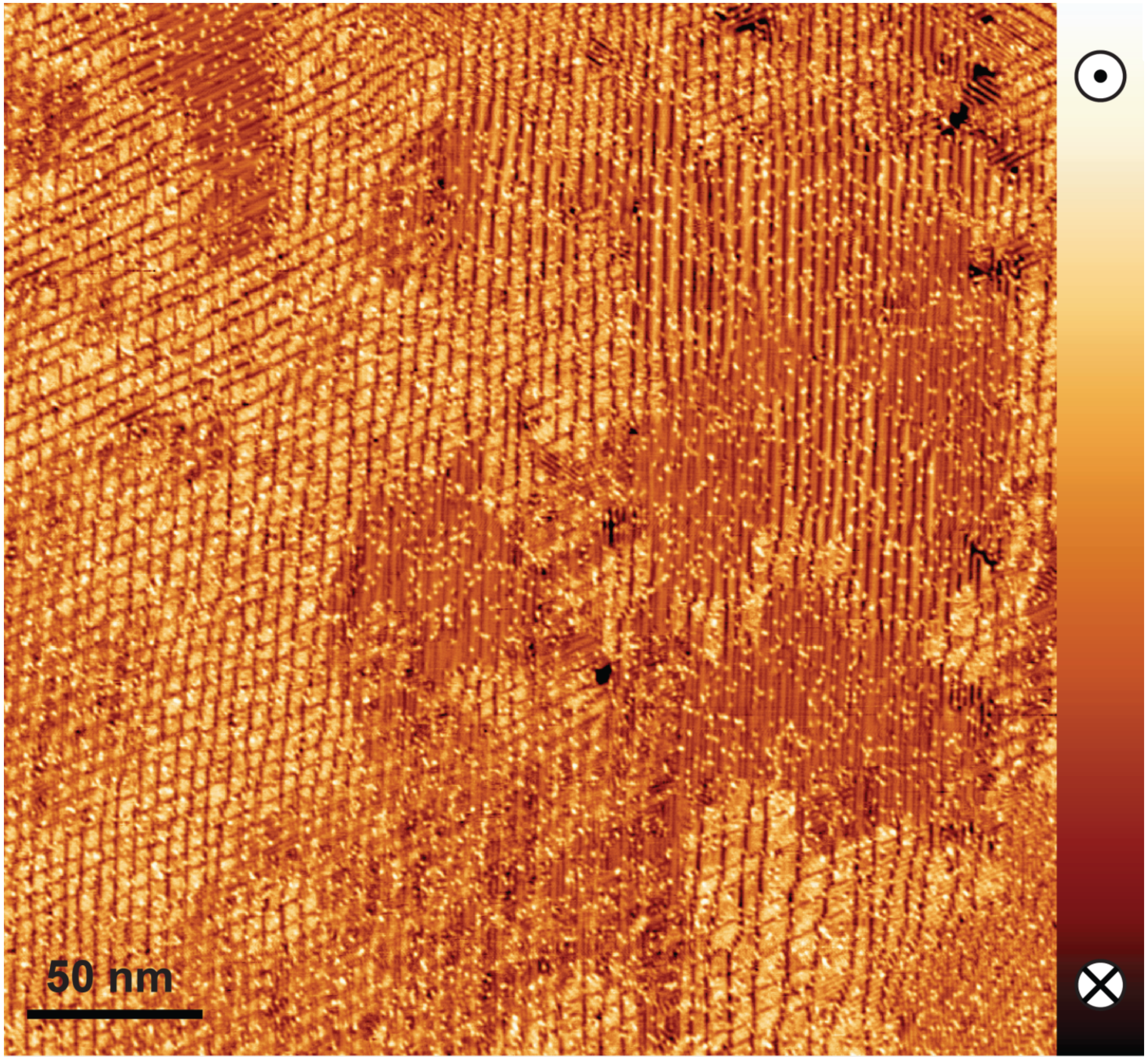

Cr bulk tip

T: 1.3K
B: 0T

✔ Short-range non-collinear order

✖ Long-range order

Magnetic structure: local correlations

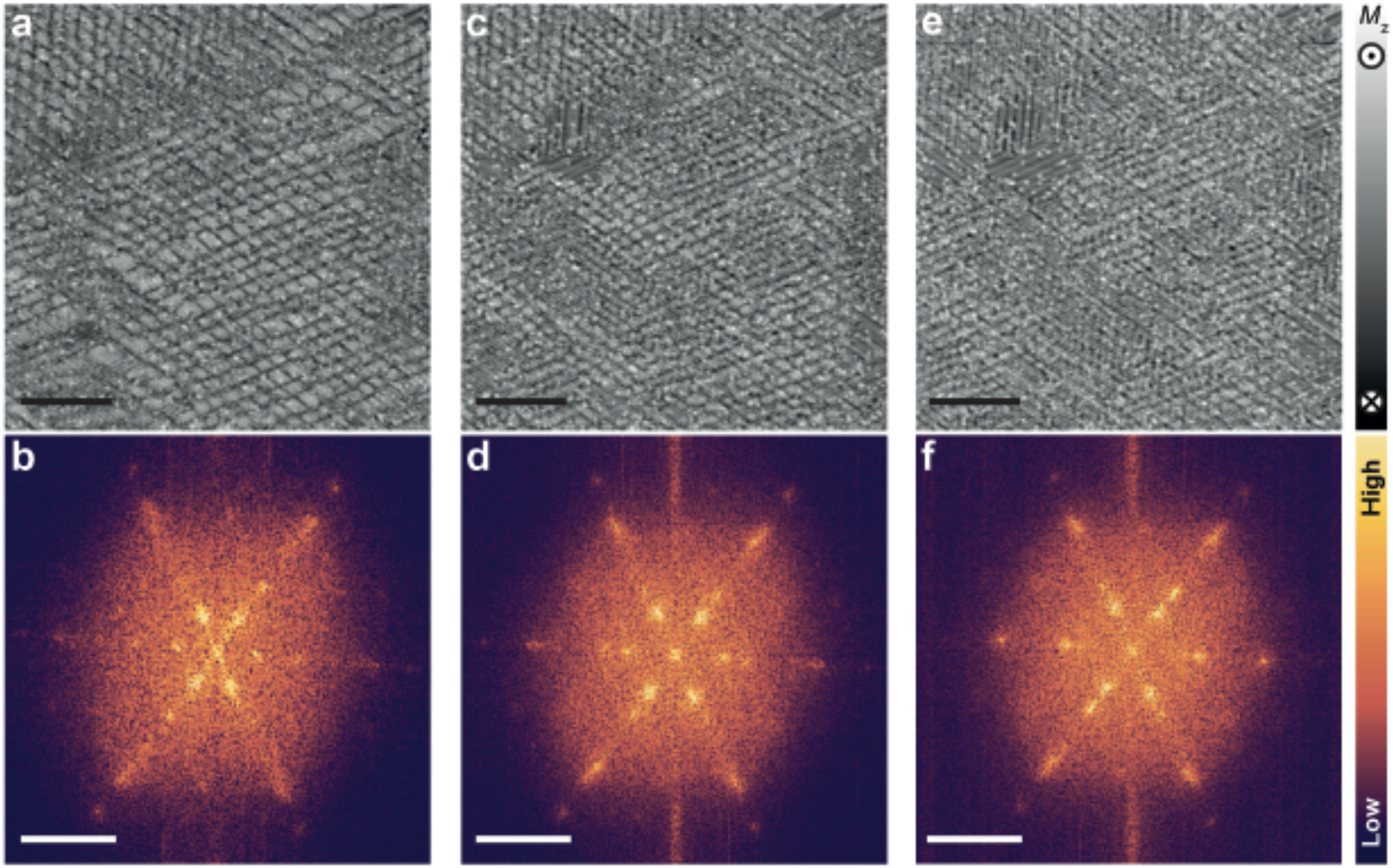

The most important observation: aging. At thermocycling (or cyling magnetic field) the magnetic state is not exactly reproduced

Ab initio: magnetic interactions in bulk Nd

Method: magnetic force theorem (Lichtenstein, Katsnelson, Antropov, Gubanov JMMM 1987)

Calculations: Uppsala team (Olle Eriksson group)

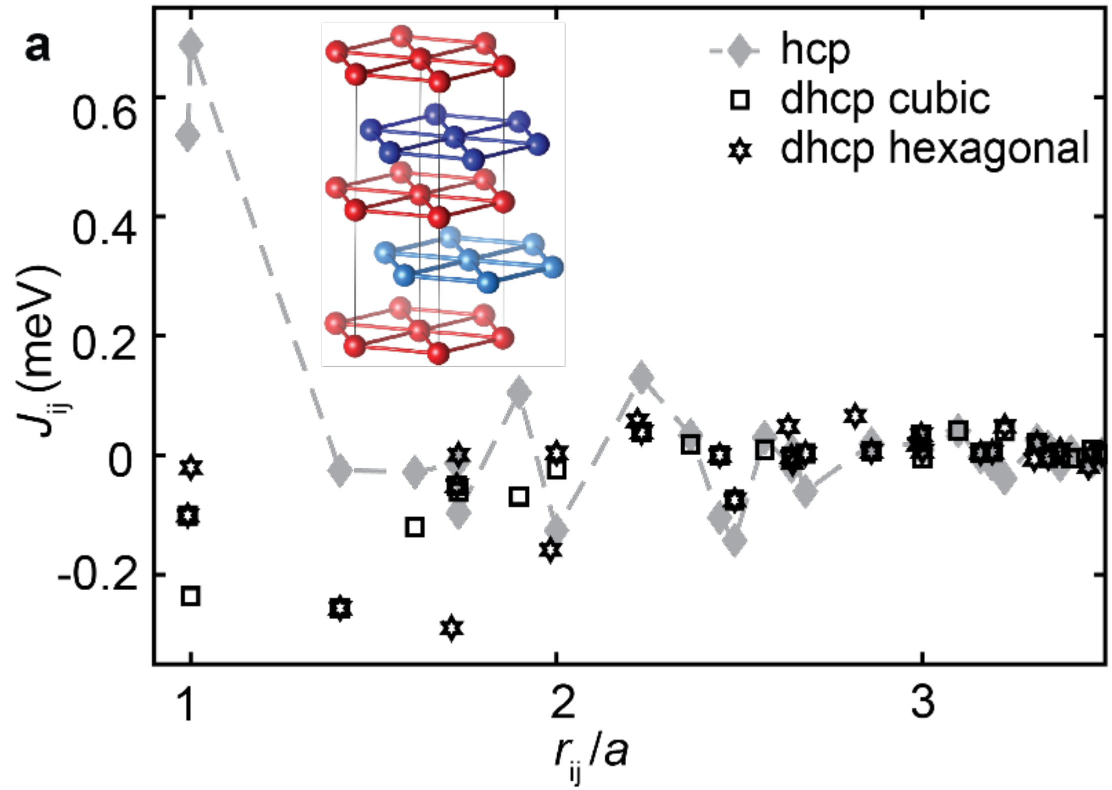

- Dhcp structure drives competing AFM interactions
- Frustrated magnetism

Ab initio bulk Nd: energy landscape

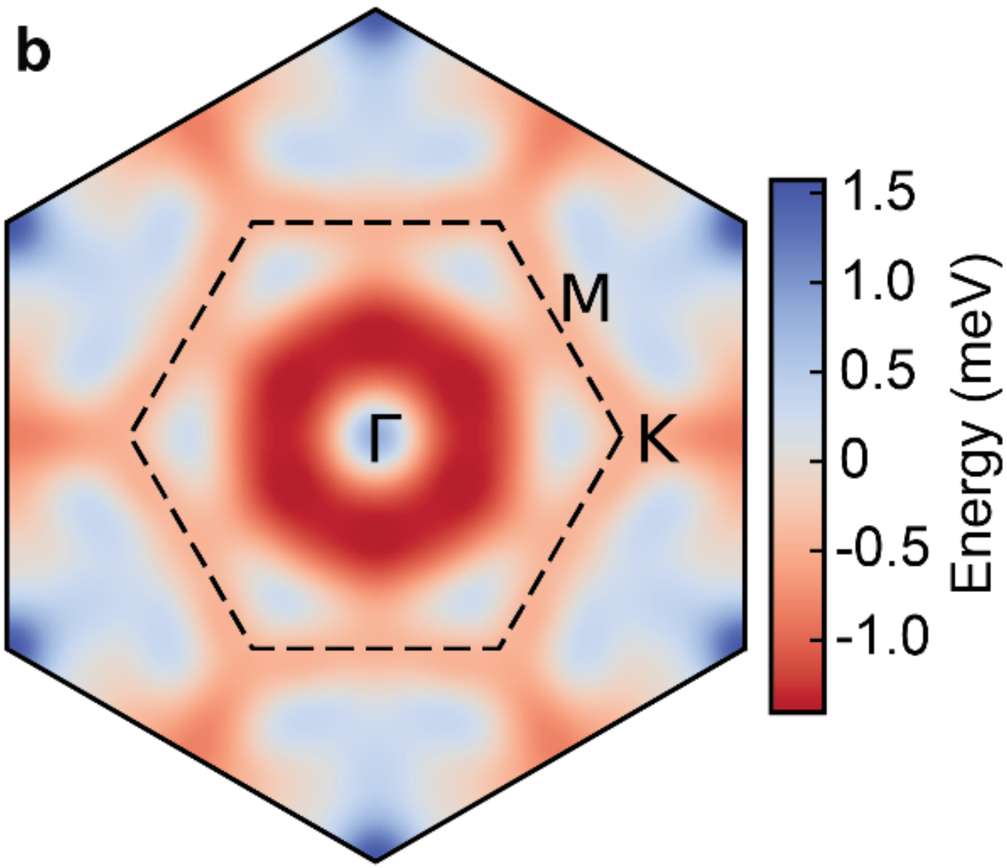

- *E*(Q) landscape features flat valleys along high symmetry directions

See A. Principi, M.I. Katsnelson, PRB/PRL (2016)/(2017)

Spin-glass state in Nd: spin dynamics

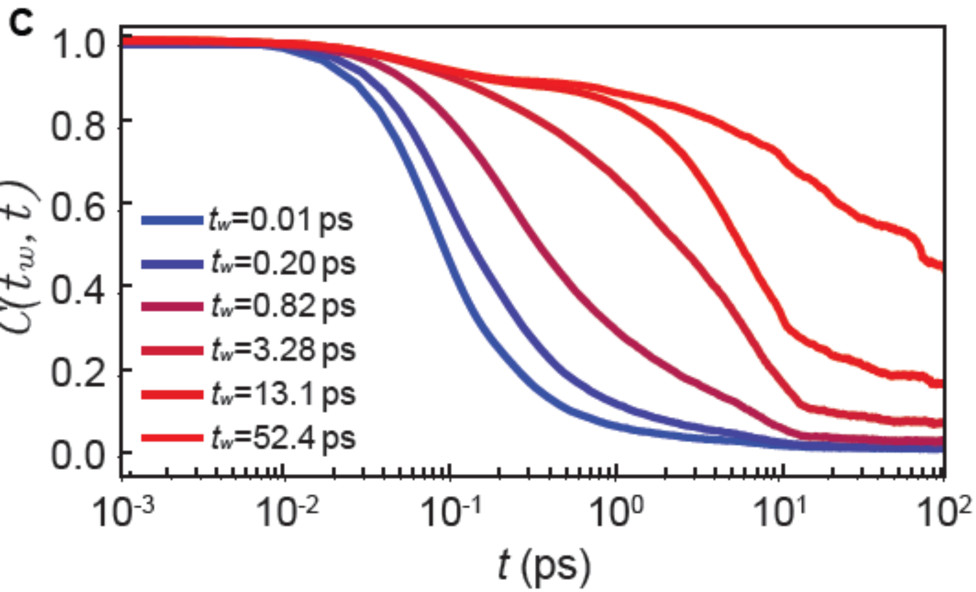

Atomistic spin dynamics simulations

Typically spin-glass behavior

Autocorrelation function $C(t_w, t) = \langle \boldsymbol{m}_i(t + t_w) \cdot \boldsymbol{m}_i(t_w) \rangle$ for dhcp Nd at T = 1 K

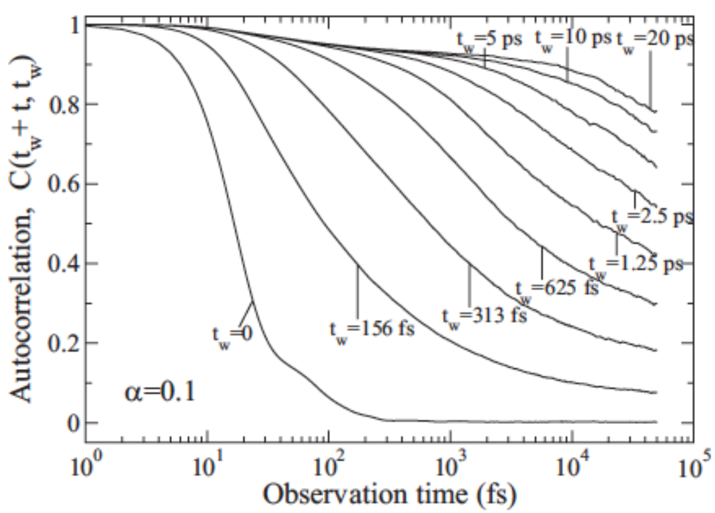

To compare: the same for prototype *disordered* spin-glass Cu-Mn

B. Skubic et al, PRB 79, 024411 (2009)

Does self-induced glassiness solve the problem?

No! **There is no real memory in spin glasses: too many local minima, too small basin of attraction of each minimum**

A hypothesis (MIK, Y. Wolf, E. Koonin, Phys. Scr. 93 (2018) 043001):
States that an "glue" not to maroscopically large number of configurations (like in glasses) and not just to a few (like for conventional broken symmnetry) but something in between:

$$H[\phi(x)] \to H_g[\phi(x)] = H[\phi(x)] + \frac{g}{2}\int dx[\phi(x) - \sigma(x)]^2$$

$$\lim_{g\to+0}\lim_{V\to\infty}\frac{F_g}{V} \neq \lim_{V\to\infty}\lim_{g\to+0}\frac{F_g}{V}$$

for many, but not too many configurations $\sigma(x)$

(in the context of "physical mechanisms of biological evolution")

Multi-well "memory" state in Ising spin systems

Atom-by-atom construction of attractors in a tunable finite size spin array

A Kolmus[1], M I Katsnelson[2], A A Khajetoorians[2] and H J Kappen[1]

New J. Phys. 22 (2020) 023038

2D Ising model, square lattice, no disorder but frustrations due to oscillating character of exchange interactions (2D RKKY)

$$H = -\sum_{i>j} J_{ij} s_i s_j;$$

$$J_{ij} = \begin{cases} 0 & , i = j \\ \frac{1}{r_{ij}^2} \sin\left(\frac{2\pi}{\lambda} r_{ij}\right) & , i \neq j \end{cases}$$

the ratio $\alpha = \lambda/a$ between the RKKY wavelength (λ) and the lattice constant (a)

is the only relevant parameter in the model

Multi-well "memory" state in spin systems II

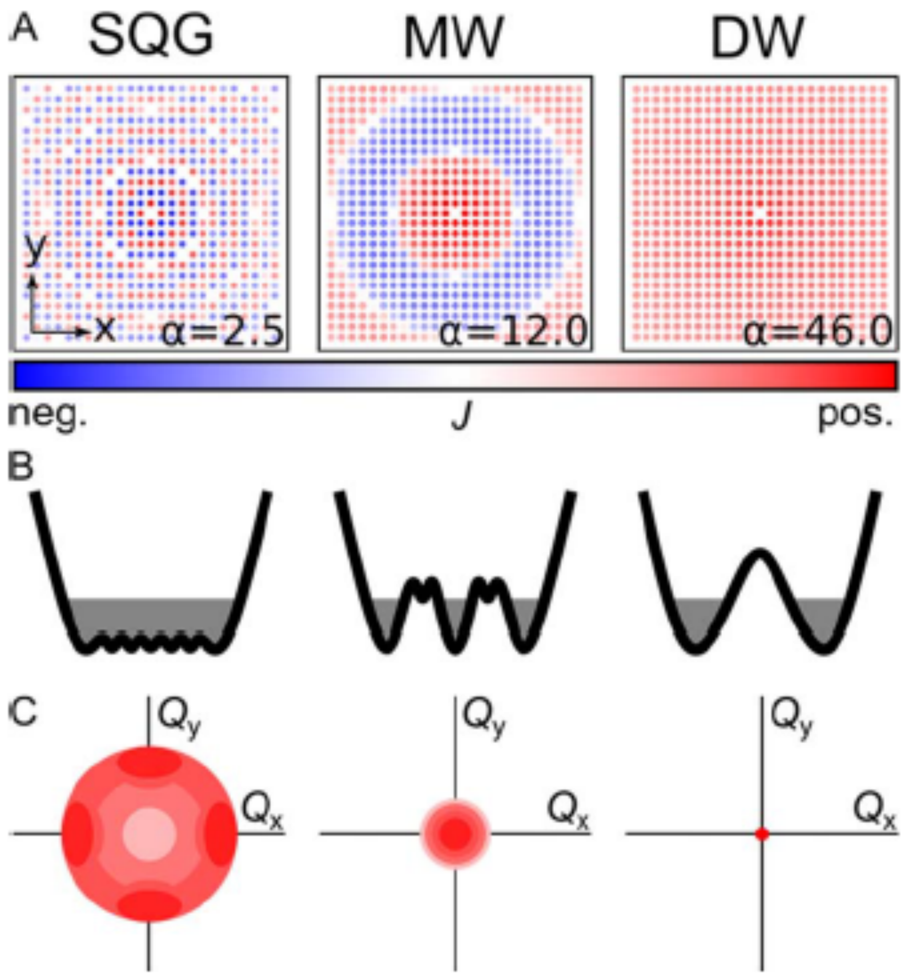

Figure 1. (a) The spatial distribution of the RKKY exchange interaction (J) for the central atom in the Ising spin array ($n = 25$) for different α for the labeled magnetic regime: spin-Q glass (SQG), multi-well (MW), double well (DW). The color bar represents the amplitude and sign of the interaction. (b) Schematic of the energy landscape for the three-labeled regimes, illustrating qualitatively the distribution and depth of states for each regime where gray illustrates the effective temperature. (c) Illustration of the distinguishing features in the Q-space histogram identifying each regime, where white to red intensity corresponds to a low to high number of states.

Multi-well "memory" state in spin systems III

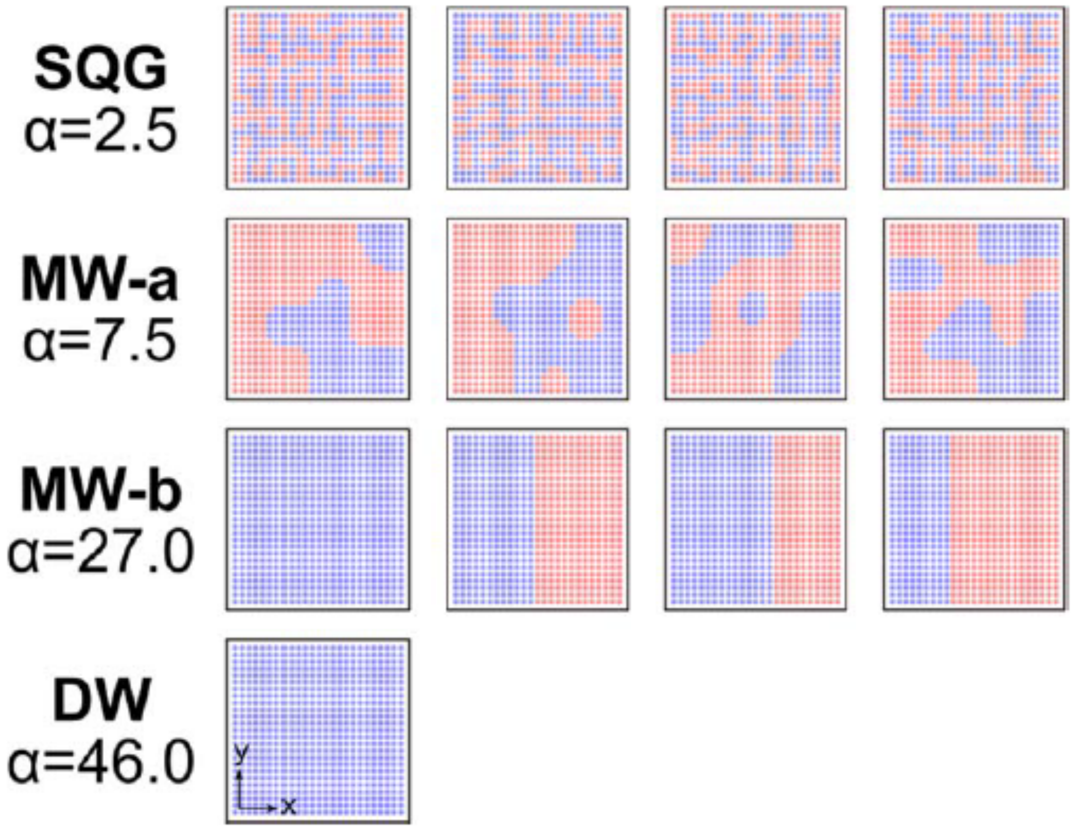

Figure 3. Examples of the real space site dependent magnetization for a lattice size of 25×25, for various metastable states for each of the labeled regimes (red/blue correspond to an average spin value of $-/+1$). Each of the patterns corresponds to a low-energy state, taken from the histogram in figure 2(b), for the labeled regime and value of α. The states increase in energy from left to right.

Multi-well "memory" state in spin systems IV

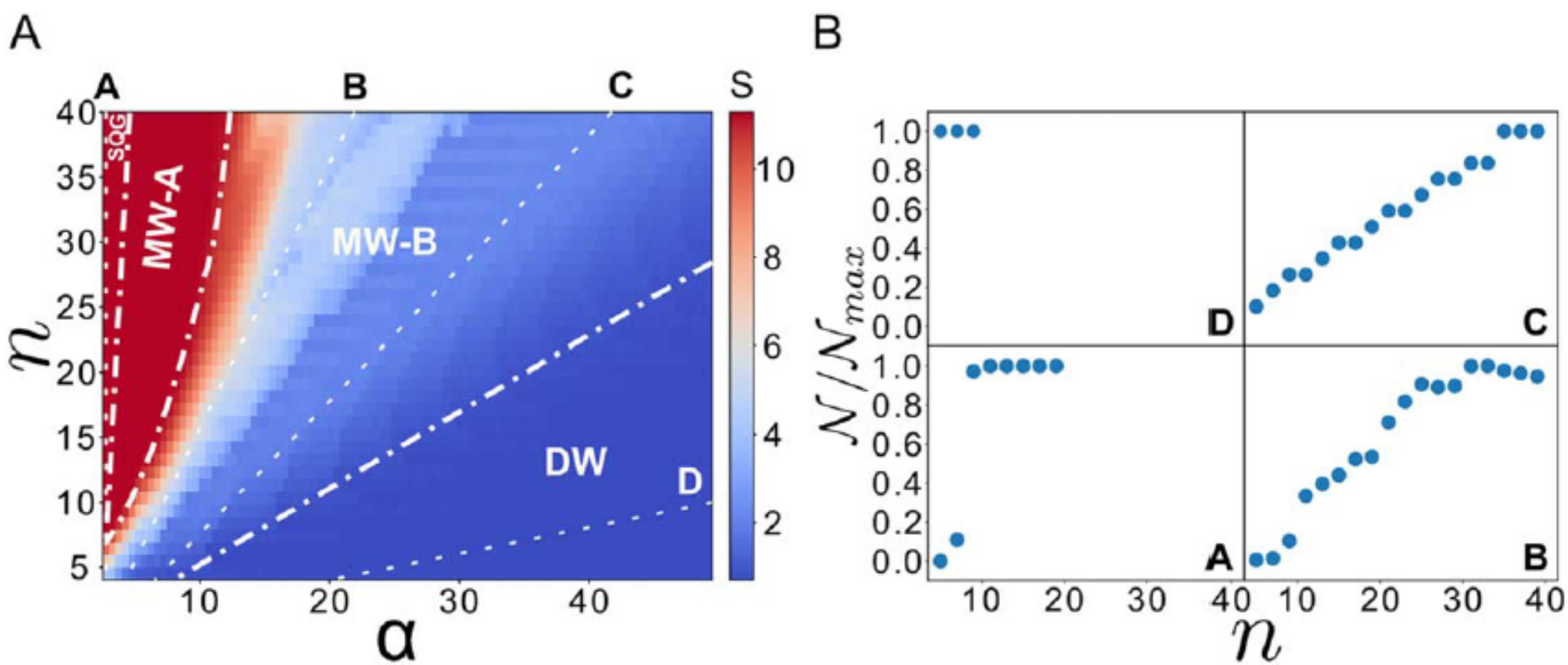

Figure 4. (a) A regime diagram with the lattice width n on the vertical axis and α on the horizontal axis. The white dashed-dot lines indicate the different regimes, as labeled and as defined by the corresponding Q-histograms. The color scale indicates the entropy as defined in the main text. (b) The scaling behavior near the boundary between each regime, corresponding to the white dashed lines in (a) and labeled by the letters A–D. Each plot corresponds to the number of available states as a function of the lattice width n versus the normalized number of metastable states N/N_{max}. N, N_{max} are the number of stable states and the largest number of stable states per graph, respectively, and we divide the former by the latter in order to normalize each plot for comparison. These simulations were repeated three times, no large differences were found.

Multi-well "memory" state in spin systems V

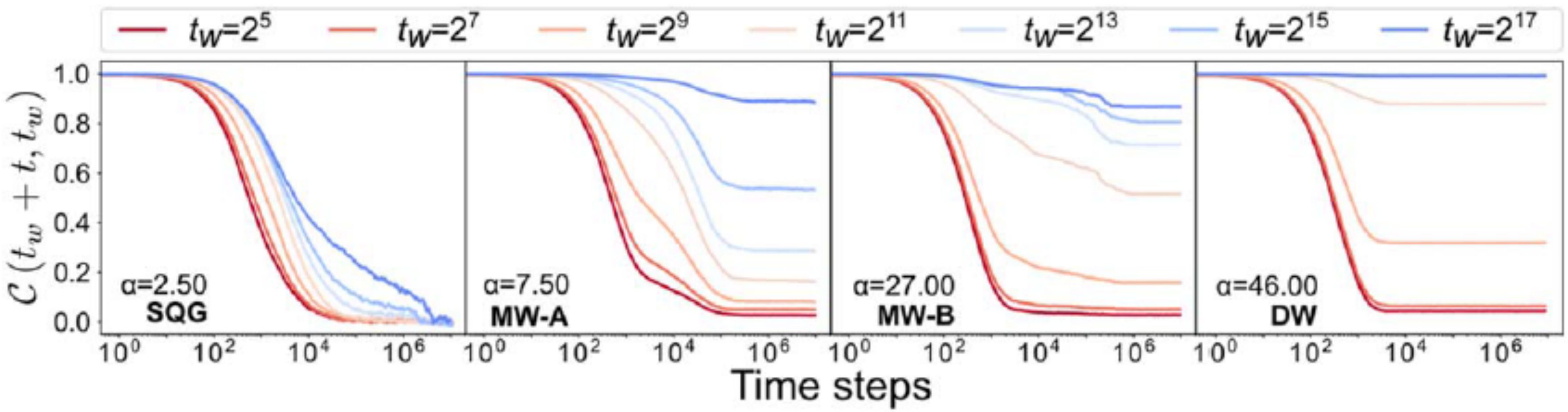

Figure 5. The autocorrelation function $C(t_w + t,\ t_w)$, as defined in the text, for different α and labeled regimes, where t_w is the waiting time before measuring the autocorrelation and t_w is the time step during the measurement as indicated by the colors/values labeled above the graphs. Each line is the average over 100 runs. For each α the temperature was set below the critical temperature (determined using the Binder cumulant), but high enough to show aging behavior in 10^7 time steps.

$$C(t_w + t,\ t_w) = \frac{1}{N}\sum_i s_i(t_w)^* s_i(t_w + t), \qquad (3)$$

Plateau in multi-well regime means memory

Frustrations and complexity: Quantum case

Generalization properties of neural network approximations to frustrated magnet ground states

NATURE COMMUNICATIONS | (2020)11:1593

Tom Westerhout[1], Nikita Astrakhantsev[2,3,4], Konstantin S. Tikhonov[5,6,7], Mikhail I. Katsnelson[1,8] & Andrey A. Bagrov[1,8,9]

How to find true ground state of the quantum system?

In general, a very complicated problem (difficult to solve even for quantum computer!)

Idea: use of variational approach and train neural network to find "the best" trial function (G. Carleo and M. Troyer, Science 355, 602 (2017))

$$|\Psi_{GS}\rangle = \sum_{i=1}^{K} \psi_i |S_i\rangle = \sum_{i=1}^{K} s_i |\psi_i| |S_i\rangle$$

Generalization problem: to train NN for relatively small basis (*K* much smaller than total dim. of quantum space) and find good approximation to the true ground state

Frustrations and complexity: Quantum case II

Quantum S=1/2 Hamiltonian
NN and NNN interactions

$$\hat{H} = J_1 \sum_{\langle a,b \rangle} \hat{\boldsymbol{\sigma}}_a \otimes \hat{\boldsymbol{\sigma}}_b + J_2 \sum_{\langle\langle a,b \rangle\rangle} \hat{\boldsymbol{\sigma}}_a \otimes \hat{\boldsymbol{\sigma}}_b$$

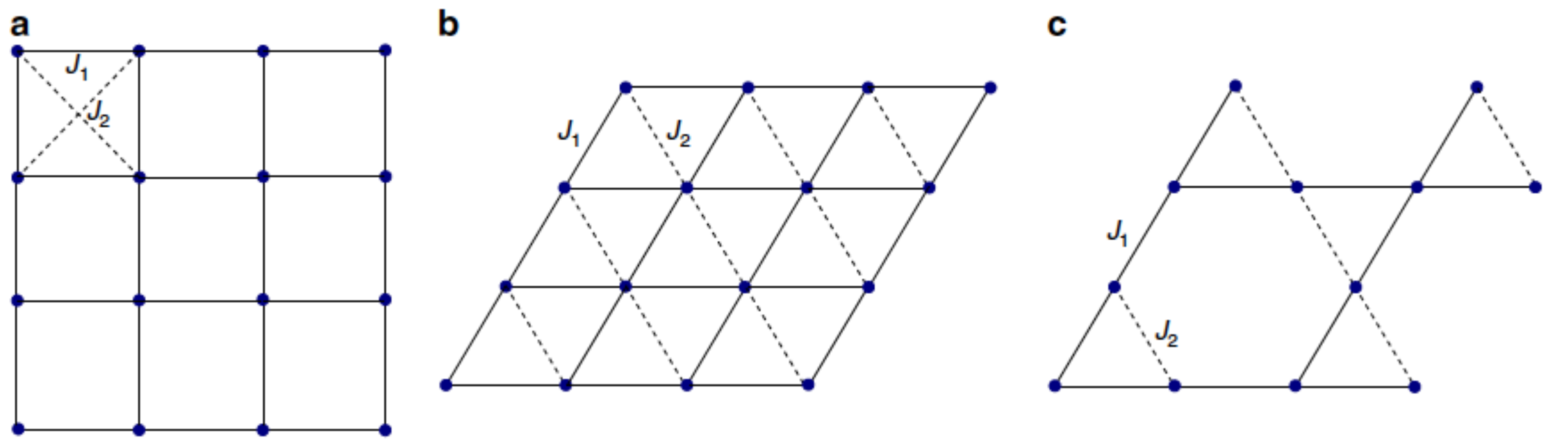

Fig. 1 Lattices considered in this work. We studied three frustrated antiferromagnetic Heisenberg models: **a** next-nearest neighbor J_1–J_2 model on square lattice; **b** anisotropic nearest-neighbor model on triangular lattice; **c** spatially anisotropic Kagome lattice. In all cases $J_2 = 0$ corresponds to the absence of frustration.

24 spins, dimensionality of Hilbert space $d = C_{12}^{24} \simeq 2.7 \cdot 10^6$

Still possible to calculate ground state exactly
Training for $K = 0.01\, d$ (small trial set)

Frustrations and complexity: Quantum case III

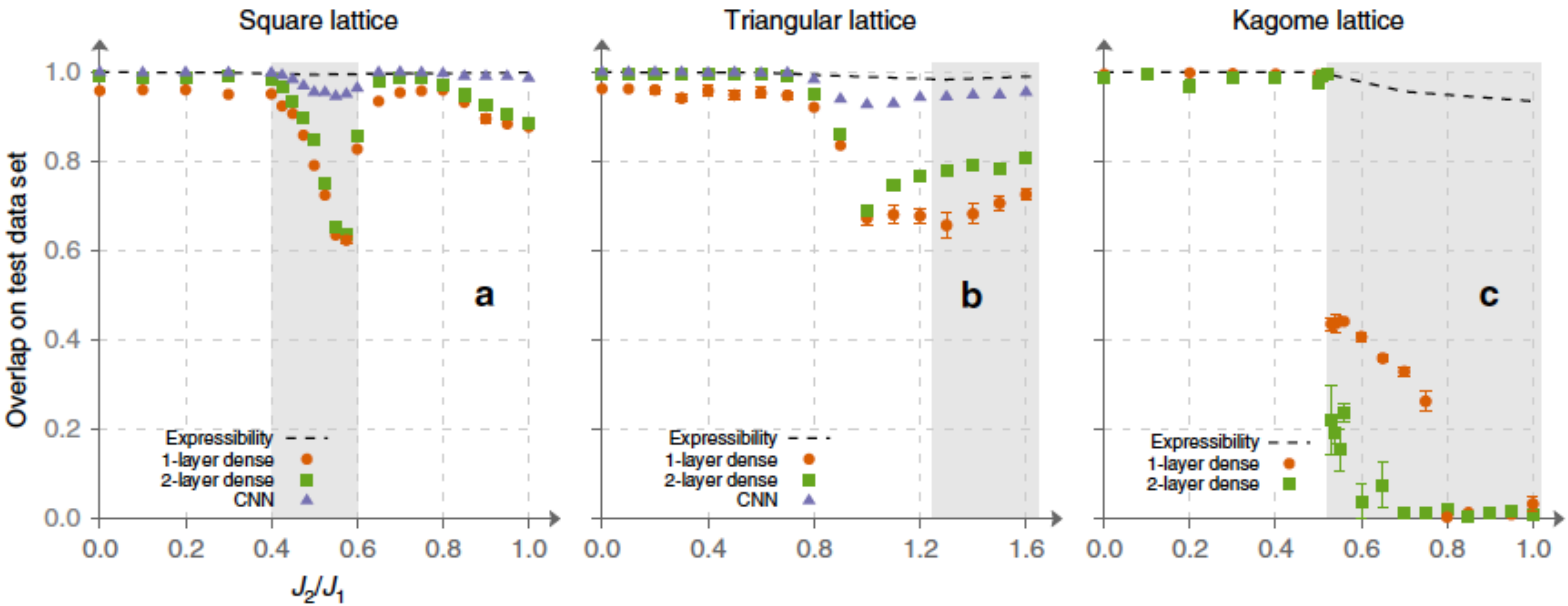

Fig. 2 Optimization results for 24-site clusters obtained with supervised learning and stochastic reconfiguration. Subfigures **a–c** were obtained using supervised learning of the sign structure. Overlap of the variational wave function with the exact ground state is shown as function of J_2/J_1 for square **a**, triangular **b**, and Kagome **c** lattices. Overlap was computed on the test dataset (not included into training and validation datasets). Note that generalization is poor in the frustrated regions (which are shaded on the plots). 1-layer dense, 2-layer dense, and convolutional neural network (CNN) architectures are described in Supplementary Note 1. Subfigures **d–f** show overlap between the variational wave function optimized using Stochastic Reconfiguration and the exact ground state for square, triangular, and Kagome lattices, respectively. Variational wave function was represented by two two-layer dense networks. A correlation between generalization quality and accuracy of the SR method is evident. On this figure, as well as on all the subsequent ones (both in the main text and Supplementary Notes 1 and 2), error bars represent standard error (SE) obtained by repeating simulations multiple times.

Frustrations and complexity: Quantum case IV

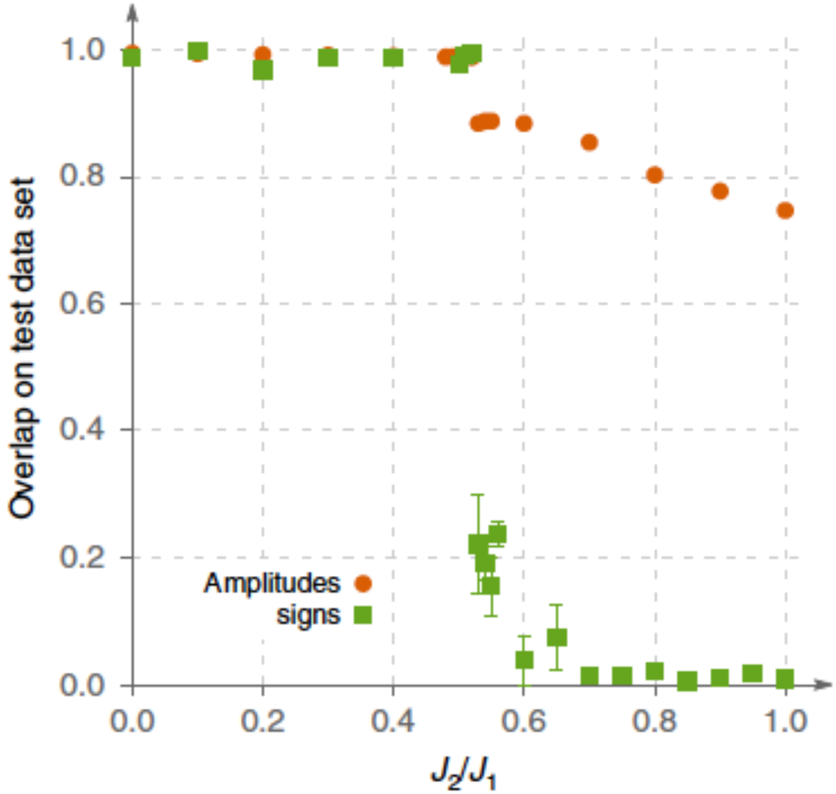

Fig. 4 Generalization of signs and amplitudes. We compare generalization quality as measured by overlap for learning the sign structure (red circles) and amplitude structure (green squares) for 24-site Kagome lattice for two-layer dense architecture. Note that both curves decrease in the frustrated region, but the sign structure is much harder to learn.

It is *sign* structure which is difficult to learn in frustrated case!!!

Relation to sign problem in QMC?!

"Somehow it seems to fill my head with ideas –only I don't exactly know what they are!" (Through the Looking-Glass, and What Alice Found There)

Frustrations and biological complexity

Physical foundations of biological complexity

Yuri I. Wolf[a], Mikhail I. Katsnelson[b], and Eugene V. Koonin[a,1]

E8678–E8687 | PNAS | vol. 115

Competing interactions as universal mechanism of complexity?!

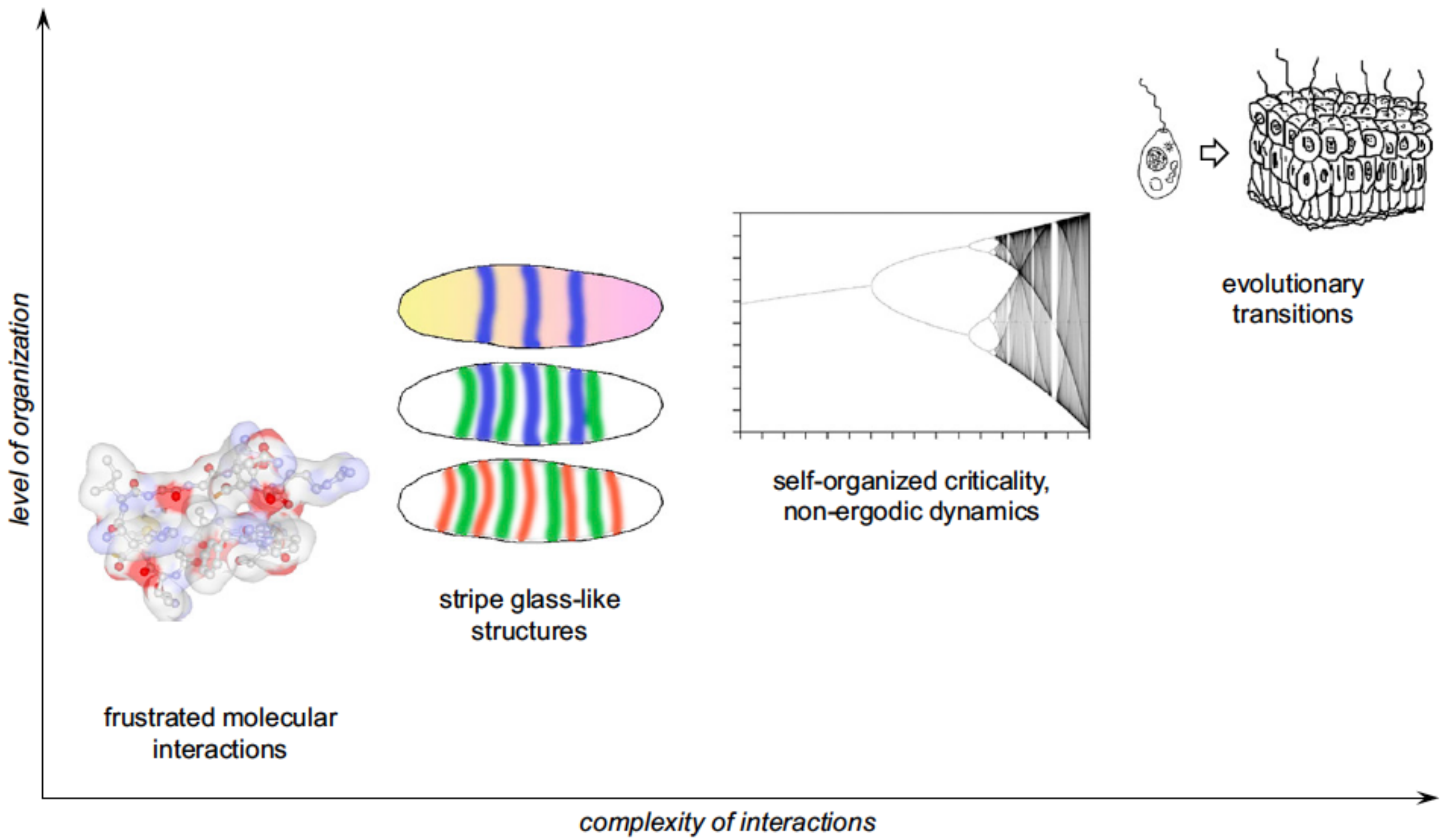

Frustrations and biological complexity II

Table 1. Competing interactions and frustrated states in biological evolution

System	Frustration-producing factors (competing interactions)	Emergent functional and evolutionary features
RNA	Short-range (within stem local hydrogen bonding, stacking) vs. long-range (long-distance hydrogen bonding, salt bridges) interactions between nucleotides	Complex 3D structures including ribozymes
Proteins	Short-range (Van der Waals) vs. long-range (hydrogen bonds, salt bridges) interactions between amino acid side chains	Stable conformations and semiregular patterns in protein structures; allostery enabled by transitions between energetically quasi-degenerate conformations
Macromolecular complexes	Within-subunit vs. between-subunit interactions	Elaborate complex organization, in particular nucleoproteins (ribosomes, chromatin)
Cells	**Membranes (confinement of chemicals) vs. channels/pores (transport of chemicals)**	**Compartments and cellular machinery dependent on electrochemical gradients**
Autonomous (hosts) and semiautonomous (parasites) replicators	**Replicator vs. parasite genomes**	**Self- vs. non-self-discrimination and defense; complex genomes of increasing size; primitive cells**
Autonomous (hosts) and semiautonomous (parasites) reproducers/replicators	**Host cells and viruses**	**Infection mechanisms, defense and counterdefense systems, evolutionary arms race; contribution to the origin of multicellular life forms**
Autonomous (hosts) and semiautonomous (parasites) reproducers/replicators	Host cells vs. transposons	Intragenomic DNA replication control; evolutionary innovation through recruitment of transposon sequences
Autonomous (hosts) and semiautonomous (parasites) reproducers/replicators	Host cells vs. plasmids	Beneficial cargo genes, plasmid addiction systems, efficient gene exchange and transfer mechanisms
Emerging eukaryotic cells	**Host (archaeal) cells vs. endosymbiont (α-proteobacteria, protomitochondria)**	**Eukaryotic cells with complex intracellular organization**
Communities of unicellular organisms	**Individual cells vs. cellular ensembles**	**Information exchange and quorum sensing mechanisms; replication control, programmed cell death, multicellularity**
Multicellular organisms	Soma vs. germline	Complex bodies, tissues and organ differentiation, sexual reproduction
Multicellular organisms	Dividing vs. quiescent cells	Aging, cancer, death
Populations	**Individual members vs. groups**	**Population-level cooperation; kin selection; eusocilaity**
Populations	Males vs. females (partners with unequal parental investment)	Sexual selection, sexual dimorphism
Ecosystems	Species in different niches	Interspecies competition, host–parasite and predator–prey relationships, mutualism, symbiosis
Societies*	—	—

Those competing interactions and frustrated states that are deemed to directly contribute to MTE are shown in bold.
*We refrain from specifying the conflicts that drive the origin and evolution of human societies.

To summarize: How it was in 1960th-1980th

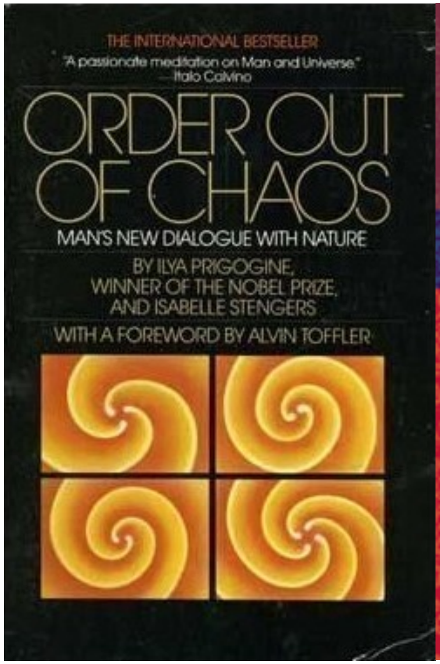

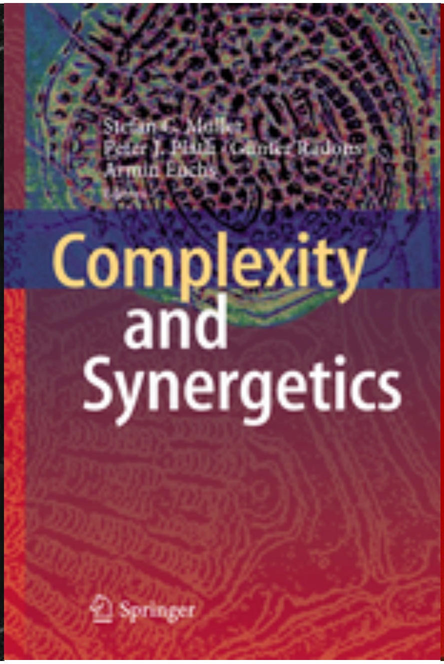

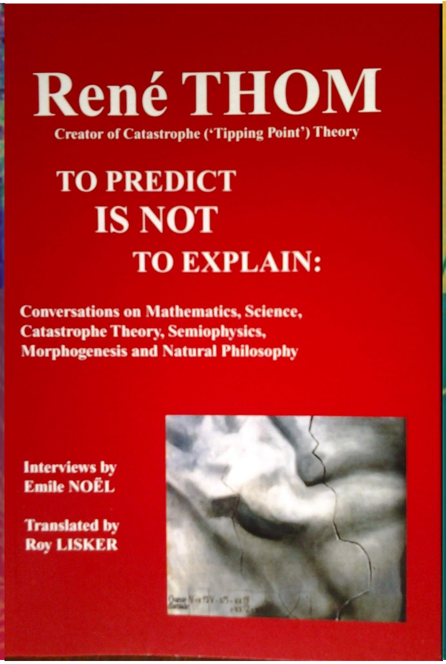

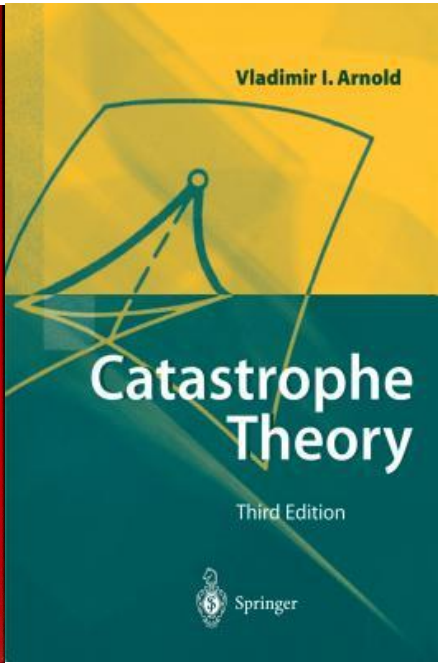

People were very enthusiastic on applications of theory of dynamical systems: attractors, bifurcations, catastrophes – useful for sure but…

The distance from Benard convection cells to origin of life seems to be too far…

To summarize: Now

Now we try statistical physics approached, our new key words are:

emergence, renormalization group flow, universality classes, spin glasses, broken replica symmetry, frustrations…

Will it help us?! Who knows...

THINK!!!